

pubs.acs.org/journal/abseba Review

Polymeric Metal Contrast Agents for T₁-Weighted Magnetic Resonance Imaging of the Brain

Dorian Foster* and Jessica Larsen*



Cite This: https://doi.org/10.1021/acsbiomaterials.2c01386

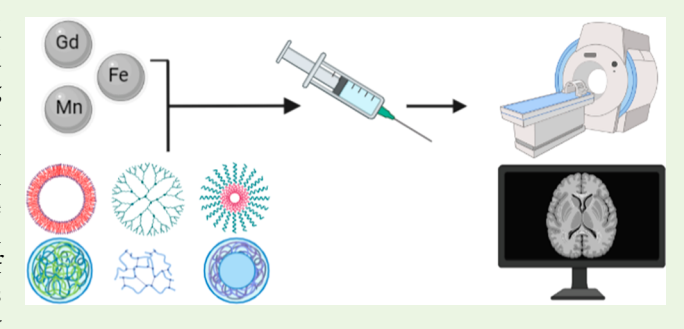


ACCESS I

Metrics & More

Article Recommendations

ABSTRACT: Imaging plays an integral role in diagnostics and treatment monitoring for conditions affecting the brain; enhanced brain imaging capabilities will improve upon both while increasing the general understanding of how the brain works. T₁-weighted magnetic resonance imaging is the preferred modality for brain imaging. Commercially available contrast agents, which are often required to render readable brain images, have considerable toxicity concerns. In recent years, much progress has been made in developing new contrast agents based on the magnetic features of gadolinium, iron, or magnesium. Nanotechnological approaches for these systems allow for the protected integration of potentially



harmful metals with added benefits like reduced dosage and improved transport. Polymeric enhancement of each design further improves biocompatibility while allowing for specific brain targeting. This review outlines research on polymeric nanomedicine designs for T_1 -weighted contrast agents that have been evaluated for performance in the brain.

KEYWORDS: Magnetic resonance imaging (MRI), brain, contrast agent, polymer

INTRODUCTION

The brain is an incredibly complex organ that plays a role in every aspect of bodily function. Many conditions are known to affect it, including cancers and neurodegenerative diseases. Accurate and timely diagnosis is essential to improving therapeutic efficacy and patient outlook in any disease. Magnetic resonance imaging (MRI) is widely regarded as the best imaging modality for diagnostics and continued monitoring of soft tissue conditions, including those of the brain. However, in many cases, brain imaging requires a contrast agent. Gadoliniumbased contrast agents (GBCAs), the only contrast agents available commercially, raise concerns around toxicity; nanomedicine approaches for contrast agents show promise for improving the safety of clinically available contrast agents and for including additional functionality into their designs. Nanoparticle (NP) systems exploiting the metallic properties of gadolinium, iron, or manganese have shown the most promise for contrast agent applications; those systems lending to contrast enhancement in T₁-weighted imaging are generally considered the most applicable for uses in the brain. This review will present research on polymeric NP-based T₁ contrast systems designed for magnetic resonance imaging of disease conditions within the brain.

BACKGROUND

Diseases of the Central Nervous System. The central nervous system (CNS) is composed of the brain and spinal

cord—two highly essential and highly protected structures. Knowledge gaps still exist surrounding the brain's anatomy, physiology, and general interworking. Increased understanding of brain pathology throughout disease is necessary to inform treatment for neurological conditions, of which there are over 600.¹

The brain is protected by a series of safeguards that prevent the entrance of foreign substances, which could upset homeostasis or otherwise cause damage. The most selective aspect of this system is the blood—brain barrier (BBB) which is primarily comprised of an endothelial cell (EC) lining surrounding the blood vessels that supply the brain. Tight junctions connecting the ECs create a secure seal between cells, preventing most intercellular transport into the brain. This system prevents the influx of over 98% of solutes. Although exact size constraints are disputed, it is known that only small, nonpolar, lipophilic particles can passively diffuse through the BBB into the brain. ^{2,3} The BBB acts as an interface where receptors recognize necessary substances to allow restricted, receptor-mediated

Received: November 18, 2022 Accepted: January 17, 2023



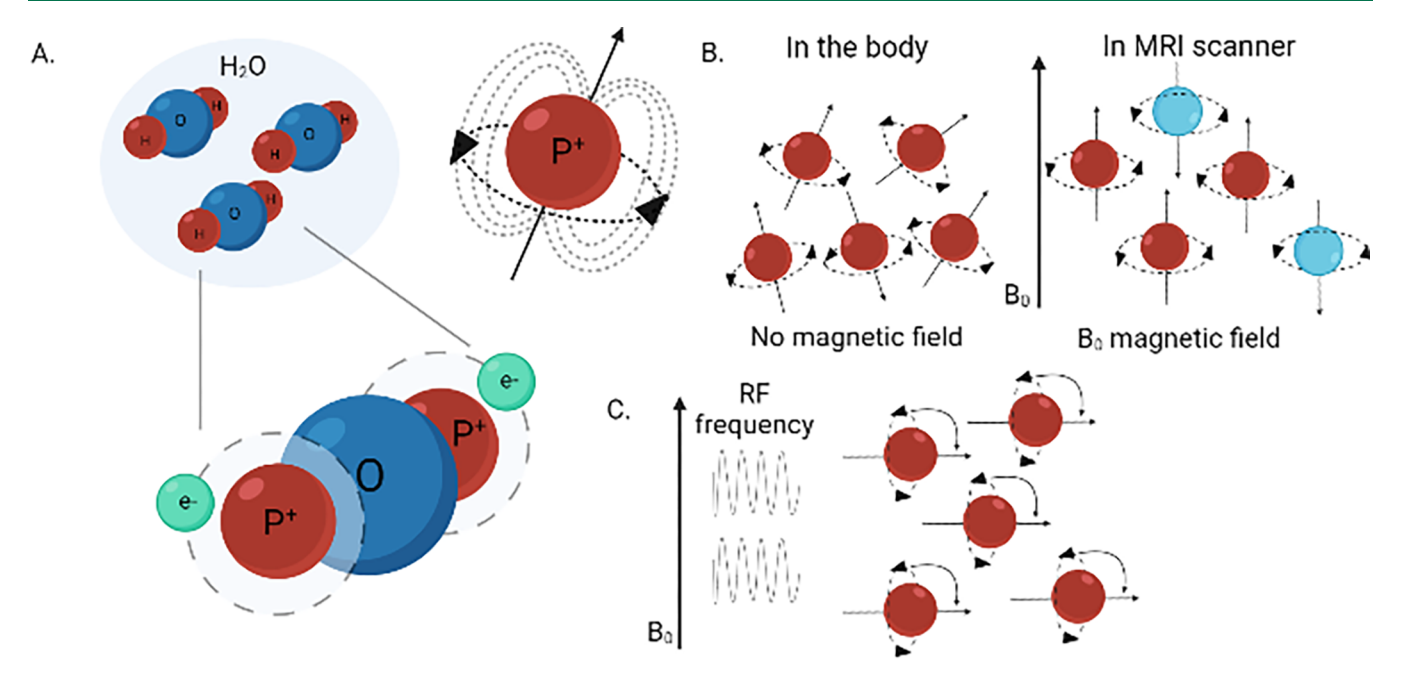


Figure 1. Proton spin in MRI. ¹² (A) Nuclear spin of a hydrogen atom in water. (B) Proton alignment with or without a magnetic field. (C) Proton response to applied RF pulse. (A–C) Adapted from ref 12. Copyright 2019 Broadhouse.

transport (RMT) for large or more complex molecules entering the brain.

The BBB must be considered in designing diagnostic or therapeutic tools for the brain. Intracerebral delivery, or injection directly into the brain, is invasive and therefore undesirable. The ideal delivery method would be intravenous (IV), or injection into the bloodstream. A variety of strategies could make a drug system IV compatible for brain delivery, including small size or conjugation with targeting moieties that will be recognized by receptors on ECs for RMT. In particular diseases, the BBB becomes disrupted and leaky; stroke, Alzheimer's Disease (AD), and Parkinson's Disease (PD) are all known to result in a compromised BBB.4 While this is dangerous for the maintenance of normal brain conditions and function, it makes brain delivery a more minor hurdle for delivery vehicle design. In any case, understanding the BBB and how it functions with respect to the disease state and the delivery system is essential to a successful design.

Adding to the challenge of diagnostic and therapeutic drug design is the fact that hundreds of brain-afflicting conditions exist, and their mechanisms and manifestations can be incredibly similar in some ways while drastically different in others. Diseases affecting the brain can have a wide range of symptoms and severity.

There is a tremendous demand for improved therapeutics and diagnostics for all brain diseases; an in-depth understanding of the brain and how it functions in a diseased state is the key to making necessary advancements. One of the strategies for expanding knowledge of the brain is improving imaging capabilities. Sophisticated visualization of the brain results in a more comprehensive understanding of individual brain diseases.

Magnetic Resonance Imaging. Since its first clinical application in 1980, magnetic resonance imaging (MRI) has become the top choice among noninvasive imaging techniques. It offers high spatial and temporal resolution and can image large portions of the body at nearly any angle. The primary shortcoming associated with MRI is lower sensitivity than other imaging techniques. MRI does not use ionizing radiation

and is, therefore, considered to be the most risk-free imaging option, especially for conditions that may require repeated imaging. Extended exposure to ionizing radiation, as employed in X-rays, computed tomography (CT), and positron emission tomography (PET), can lead to cancer development. MRI instead uses strong magnetic fields to procure a three-dimensional image based on the intrinsic magnetic properties of the atoms that make up the human body.

Protons, electrons, and neutrons each possess an intrinsic property called "spin," the strength and direction of which are responsible for its magnetic and electrical properties. The summation of spins from protons and neutrons, both of which are housed in the nucleus, yields the nuclear spin. The nuclear spin is the nucleus's magnetic moment and is what causes nuclei to interact with magnetic fields. Not all atoms exhibit a net nuclear spin; hydrogen atoms do. Hydrogen comprises only one proton; with only a single spinning body, the nucleus does not experience competitive influence from other nuclear bodies, so its nuclear spin is effectively the same as that of the proton.

Hydrogen is abundant in the body and is found in water and other naturally occurring compounds. The hydrogen atoms in water are the primary nuclei imaged with MRI. The generation of magnetic resonance (MR) images relies on water content, making MRI best suited to imaging soft tissues, such as muscles or organs, including the brain, due to their high water content.

In MRI, a strong magnetic field B_0 is applied, which causes hydrogen protons in water molecules to align axially with the field, either in parallel or perpendicularly. In clinical applications, this field generally has a strength of 0.5 to 3.0 T, with a higher strength allowing for more detailed images; for research purposes, much higher strength scanners are available. A second magnetic field, B_1 , is then applied perpendicular to the static field at a different radio frequency (RF). As a result of the second magnetic field, the protons absorb energy, become excited, and experience an altered spin away from their equilibrium with B_0 . The second magnetic field is usually applied in short pulses, lasting only microseconds. When B_1 is turned off, the protons relax and return to equilibrium, releasing

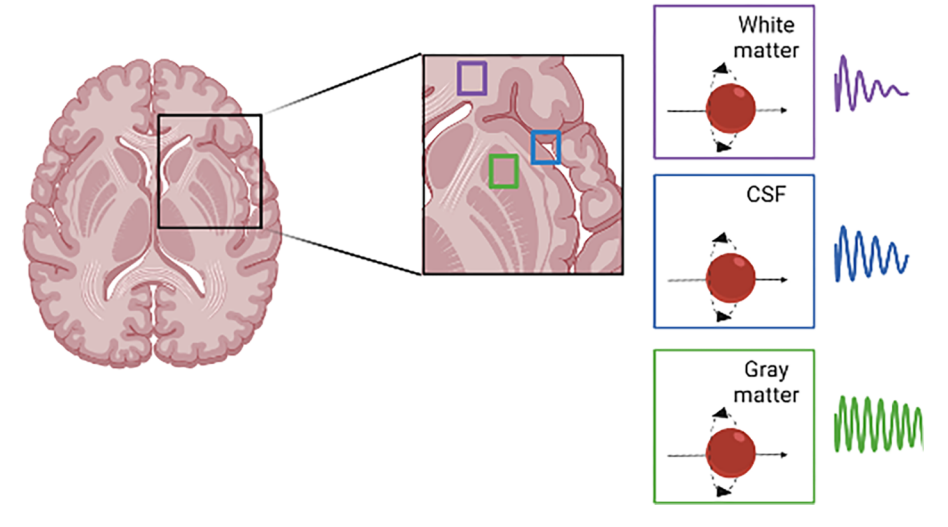


Figure 2. Signal variation in brain tissue. 12 Adapted from ref 12. Copyright 2019 Broadhouse.

the previously absorbed energy. Figure 1 gives a schematic representation of the proton spin activity involved in MRI. The energy change generated with each pulse emits a signal detected by magnetic sensors. The signals are averaged with respect to relaxation time before being mathematically transformed into an image. 11

Relaxation time, or time taken for equilibrium to be reestablished, is quantified in two ways-longitudinal and transverse relaxation times, or T_1 and T_2 , respectively. T_1 is a measure of how long it takes for the longitudinal magnetic vector to return to its equilibrium state, specifically the time at which the longitudinal magnetization has returned to 63% of its equilibrium value. At equilibrium, longitudinal magnetization is at a maximum. T2 is a measure of how long it takes for the traverse components of magnetization to dephase, specifically the time at which the traverse magnetization value has returned to 37% of its equilibrium value. Relaxation time is a function of magnetic field inhomogeneity, as well as the magnetic properties of the particle; those magnetic properties can, in turn, be influenced by particle size, shape, composition, morphology, and more. 13 T_1 and T_2 are tissue specific but T_1 is always shorter than T_2 .¹⁴

Different types of images can be generated by adjusting the sequencing parameters, repetition time (TR), and time to echo (TE). TR is the time between pulses applied to the same region, while TE is the time between the RF pulse and the detection of the resulting signal. 15 The two most common MRI sequences are used to create T₁-weighted or T₂-weighted images. T₁weighted images are derived from T₁ relaxation, meaning that the contrast in the image is determined predominantly by T₁ properties, while T₂-weighted images are derived from T₂ relaxation time. T₁-weighted images use short TR and short TE; T₂-weighted images use longer TR and TE. T₁ and T₂weighted images can be easily differentiated by how different tissues appear which is a result of signal intensity. On MR images, low-intensity signals appear dark, and high-intensity signals appear bright. Signal intensity relies on proton density, the difference in water content between tissues, and relaxation time. Differences in these properties generate the contrast required to yield a readable image with differentiable structures, as exampled by Figure 2. Water and CSF appear dark on T₁weighted images while fat appears bright; on T2-weighted images, the opposite is true.

 T_1 and T_2 images can both be valuable options for matters of the CNS. However, based on the better readability achieved by a brighter image, T_1 -weighted images tend to be preferred. ^{16–18}

Contrast Agents. While MRI is a valuable imaging tool for various applications, in about 25% of MRI procedures in the brain and spinal cord the natural tissue-to-tissue contrast is insufficient to yield a readable image, ¹⁹ necessitating the use of contrast agents (CAs). Most risks associated with MRI have to do with potential allergic reactions or toxicity caused by the CA. However, CAs are still necessary for many instances to compensate for the lower sensitivity of MRI. Figure 3 gives an

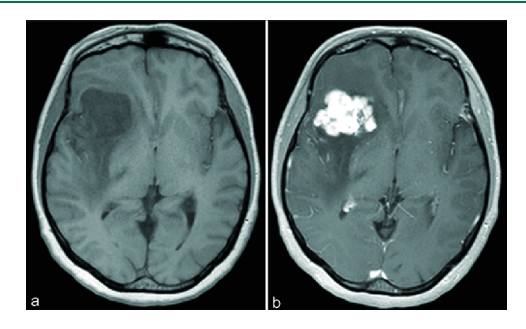


Figure 3. T₁ MR image of a brain with a fibromyxoid tumor (a) without contrast (b) with contrast. ²⁰ Reproduced with permission from ref 20. Copyright 2021 Surgical Neurology International.

example of a T₁-weighted MR image of a tumor-afflicted brain before and after administration of a CA. Most CAs work indirectly, with the agents themselves not detected by MRI but instead enhancing image contrast due to their interactions with the surrounding tissue.

The majority of CAs are relaxation agents, or agents that alter the relaxation rate $(T_1^{-1} \text{ or } T_2^{-1})$ of water in tissue. ²¹ CAs are typically paramagnetic or superparamagnetic metals. Paramagnetism is a phenomenon in which an atom has a net magnetic field of zero when under no applied magnetic field. Paramagnetic particles exhibit a positive magnetic susceptibility, ²² meaning that magnetic fields are strengthened in the presence of that material. Paramagnetic substances reduce T_1 and T_2 relaxation times in surrounding tissues, but T_1 effects often predominate. Paramagnetic contrast agents are, therefore, most applicable on T_1 -weighted images, where a brightening

effect results from their presence; CAs of this type are referred to as T_1 contrast agents. Superparamagnetism is similar to paramagnetism, with superparamagnetic substances even more susceptible to magnetization by external magnetic fields. Superparamagnetic substances decrease the T_2 relaxation time primarily, making images darker where they accumulate, and are mostly used as T_2 CAs.

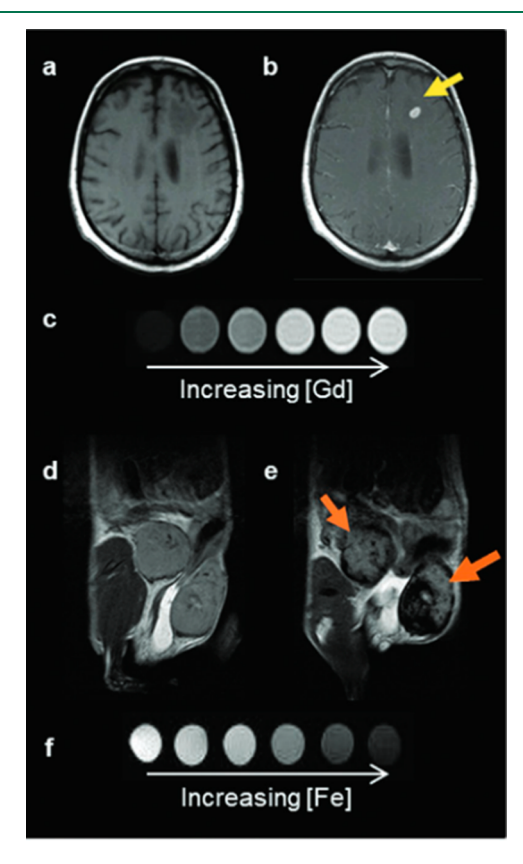


Figure 4. Comparison of MRI CAS. (a) Pre- and (b) post-GBCA T_1 enhancement of brain metastasis. (c) Brightness effects on T_1 images with Gd concentration. ²³ (d) Pre- and (e) post-IONP T_2 enhancement of mammary tumors. (f) Darkening effects on T_2 images with Fe concentration. ²⁴ Reproduced from ref 77.

Relaxation²⁵ agents are most often described in terms of relaxivity, r_i (i = 1, 2), which quantifies the extent to which the CA affects proton relaxation time; this paper will discuss relaxation CAs exclusively and will therefore refer to them only as CAs.

Contrast enhancement is linearly related to the concentration of CA. Relaxivity, then, is the slope of the plot of T_1^{-1} or T_2^{-1}

versus concentration. ²⁶ The relaxivity ratio, r_2/r_1 , helps evaluate a CA's aptitude for use as either a T_1 or T_2 CA. CAs with low r_2/r_1 values (less than 4) are considered good candidates for enhancing T_1 -weighted images, while high r_2/r_1 values (10 or greater) suggest the best compatibility with T_2 -weighted images. ^{27,28} It is important to note when comparing different CAs that relaxivity is dependent on magnetic field strength—increasing magnetic field strength tends to decrease r_1 while increasing r_2^{29} —so direct comparisons should only be made with systems operating under the same MRI conditions.

To date, the only CAs to attain FDA approval and sustain clinical application are those based on paramagnetic agents and are T_1 CAs. Although T_2 CAs are still being researched, T_1 CAs are generally considered more desirable because contrast enhancement via brightening within an image is easier to interpret than image darkening.¹⁶

Clinical Standard of Care. Gadolinium-based contrast agents (GBCAs) are the only FDA-approved MRI contrast agents to have continued clinical use, making them the gold standard of MRI CAs. Gadolinium (Gd) is a member of the lanthanide series of metals; it has seven unpaired electrons and is paramagnetic causing it to be used exclusively as a T_1 CA.

Gadolinium is not a natural component in normal biological processes, and ionized gadolinium has been shown to be toxic in various animal studies. ²² Complexes of Gd ions and a chelating agent have demonstrated reduced toxicity to levels deemed acceptable for clinical usage. As of 2018, there are eight clinically approved GBCAs, although only five remain on the market; all utilize Gd chelates (Table 1).

GBCAs can be categorized into one of two groups based on the shape of their chelating ligand: linear or macrocyclic. Beyond these differences or differences in charge, which account for differences in relaxivity and chemical stability, 30 all GBCA forms have broadly similar structural designs and function with the same mechanism. ^{21,31} All but two clinically approved GBCAs, Ablavar and Eovist, are approved for MRI in the CNS but none are designed solely for or with brain imaging in mind specifically.31 A 2022 meta-analysis examining the use of approved GBCAs in CNS imaging saw increased diagnostic confidence in 95% of cases while noting minimal adverse effects.³² Despite these promising results, GBCAs are severely limited in applicability. GBCAs cannot cross the BBB and are only useful for CNS imaging when the BBB is compromised or leaky, which can result from diseases including multiple sclerosis, stroke, or cancer but is not characteristic of every brain disease.²¹

Although chelation has rendered GBCAs safe in most cases, the use of any GBCA is unsuitable for those with decreased kidney function. 42 Normally, Gd chelates are cleared from the

Table 1. Gadolinium-Based Contrast Agents with FDA Approval for Clinical Use³³

Drug Name	Active Ingredient	Approval Year	Market Availability	Relaxivity ^a $(mM^{-1} s^{-1})$	Chelating Form
Dotarem (Gd-DOTA) ³⁴	Gadoterate meglumine	2013		3.4-3.8	Macrocyclic
Gadevist ³⁵	Gadobutrol	2011		4.9-5.5	Macrocyclic
Ablavar ³⁶	Gadofosveset trisodium	2008	Discontinued	18-20	Linear
Eovist ³⁷	Gadoxetate disodium	2008		6.5-7.3	Linear
Optimark ³⁸	Optimark ³⁸	1999	Discontinued	4.4-5.0	Linear
Magnevist (Gd-DTPA) ³⁹	Gadopentatate dimeglumine	1998	Discontinued	3.9-4.3	Linear
Omniscan ⁴⁰	Gadodiamide	1993		4.0-4.6	Linear
Prohance ⁴¹	Gadoteridol	1992		3.9-4.3	Macrocyclic

^aMeasured at a field strength of 1.5 T.

body via renal filtration within hours of intravenous administration. For those with reduced kidney function, however, GBCAs may not be removed effectively, resulting in prolonged retention. As time in the body increases, the risk of chelate dissolution and release of the toxic Gd³⁺ increases. An additional risk for those with renal impairment is the development of nephrogenic systemic fibrosis (NSF), a novel disease associated with GBCA exposure. Since 2007, the incidence of the disease has decreased significantly due to strict adherence to updated guidelines meant to identify and protect high-risk patients. Linear chelate GBCAs are considered higher risk for the disease because the linear ligands are less strongly bonded than macrocyclic ones and offer less protection to the Gd ion.

Recently, a new concern has arisen around the repeated use of GBCAs: deposition of Gd in the brain. As evidenced by areas of high signal intensity on unenhanced T_1 -weighted MR images as well as histological analysis, Gd can be retained in the brain months to years after the administration of a GBCA. In response to these results, the FDA came out with new safety guidelines and a new class warning for the use of GBCAs in 2017. As with NSF, linear Gd chelates have been noted to present a higher risk. To date, no adverse effects have been linked to these Gd deposits, however, so the effects are still largely unknown.

The concerns around toxicity raised in recent years have invigorated research for CA alternatives. Even with toxicity concerns, GBCAs have maintained their FDA approval, albeit now with black box warnings, so for any alternative to achieve clinical approval and enter the market, it must be either noninferior or superior in terms of both safety and performance.

■ NANOMEDICINE MRI CONTRAST AGENT

Polymer Enhanced Nanotechnology. Nanotechnology has seen a sharp rise in interest in recent years across a variety of fields. Nanomedicine, the application of nanotechnology in medical settings, is incredibly promising for meeting the strict requirements of clinically aimed materials. Nanoparticles present an alternative approach for safer integration of otherwise toxic molecules and have been shown to be well-suited for the delivery of diagnostic and therapeutic tools into the brain making them attractive for use with neurologically applied CAs. 1 NPs are particles ranging from 1 to 100 nm but are highly tunable for aspects like size, shape, and composition.⁴⁷ Given that the BBB is known to have size-based limitations for transport, nanomedicine is particularly appealing for use with brain diseases. NP CAs are also thought to provide faster and deeper penetration while still being easily cleared by the kidneys, protecting the body from accumulation effects like those observed with traditional GBCAs.⁴⁸

As far as polymeric NP approaches, CAs are often encapsulated in a polymeric shell or otherwise bound to a polymer network; various polymeric nanoconstructs have been developed for these purposes (Figure 5). While all are primarily promising for their ability to decrease the cytotoxicity of free drugs, each carrier has its own set of advantages and disadvantages. Micelles and polymersomes are some of the most common polymeric carriers; both are capable of loading both hydrophilic and hydrophobic drugs. Micelles require low polymer concentrations for synthesis, but they suffer from low stability. Polymersomes have better stability and are highly tunable and easily functionalized but offer low encapsulation efficiency. Nanogels are rising in popularity due to their high loading capacity and stability while dendrimers have garnered

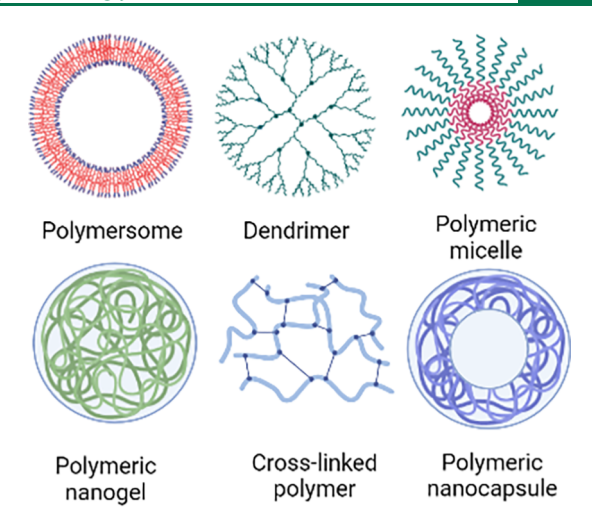


Figure 5. Common polymeric nanoconstructs.

interest for their ability to encapsulate bioactive drugs. Still, too, simple polymer conjugation to achieve a coated CA is another approach that can be seen in recent literature. The advantages and disadvantages of each polymer-based delivery system have been reviewed extensively elsewhere. 3,49–60

Polymeric NPs are especially attractive for their ability to increase biocompatibility, stability and half-life as well as integrate functionalities. Drug targeting is a functionality common in brain-specific designs that make polymeric NPs well-suited for contrast-enhanced brain imaging. Perhaps the most obvious concern with polymeric versions of CAs is the increased size as compared to traditional CAs, especially given that BBB transport is so size dependent. To bypass size limitations, transport for polymeric CAs relies heavily on brain targeting through RMT. Because polymers have high affinities for functionalization, polymeric NPs can be conjugated with targeting moieties that ensure brain internalization. 1-3,50 In some cases, the polymer itself may even serve as the targeting moiety, like with the natural polymer, hyaluronic acid, which is recognized by LDLR receptors upregulated in the brain.⁶¹ Targeted brain delivery is an improvement upon the sizedependent diffusion into the brain, anyway, because it is more specific and less susceptible to premature clearance by the liver and kidneys. 58,59 Additionally, it makes polymeric CA NPs more widely applicable as they do not depend on the leakiness of the BBB for brain entry as traditional GBCAs do.

Reduced toxicity and increased relaxivity are the two major aims of improved general CA design; the use of polymers can address both of these. Toxicity is reduced when the contrastenhancing metal or metal ion is encapsulated within or otherwise bound to a polymeric nanoconstruct as metal leakage is prevented.⁶² Polymeric CA systems have shown enhanced relaxivity values over commercial GBCAs or nonpolymeric CAs of the same kind because the polymer serves as a direct manipulation of the CA's environment. Specifically, hydrophilic polymers are desirable as they facilitate contact between water molecules and CA which increases the hydration number as well as the water retention time, both working to boost r_1 . 62-64Additionally, the size increase of the CA system due to the polymer works to slow correlation time which increases relaxivity. 63 CA aggregation within the polymeric NP has also been attributed to better contrast enhancement performance as it localizes a concentrated dosage. 60 Polymer influence on CA

relaxivity is further tunable through manipulation of factors like amino acid sequence ⁶⁵ and molecular weight. ⁶⁴

Another challenge that must be addressed with polymeric CAs is the potential toxicity of the polymer itself. Polymer choice is paramount to biocompatibility. As with any biomaterial, the host's response, behavior in the body, and degradation products of the foreign body must all be considered and the material and its properties must be matched to its function and target environment.⁵⁷ A polymer that is not sufficiently biocompatible can trigger a host of undesired responses including infection, blood clotting, and inflammation response. Biocompatible polymers can be synthetic or natural or a combination thereof. Biomimetic and biodegradable polymers are more advanced approaches at biocompatibility and have shown promise in biomaterials and carrier-mediated drug delivery applications. Polymer properties like surface composition, hydrophilichydrophobic character, and topography (among others) can all affect cytotoxicity; likewise, characteristics like the size and shape of a polymeric nanoparticle also play a role. Several biopolymers have clinical approval for use in controlled drug delivery devices but each has its own advantages and disadvantages. 66 These polymers, or chemically similar ones, tend to receive the most attention for application in new devices such as with CAs. Biocompatibility of a given polymer can be further improved by mechanical or physiochemical surface modifications. In vitro and in vivo evaluation of all components of a polymeric CA NP (CA, polymer, conjugated ligands, etc.) is necessary to screen biocompatibility.

Polymers are incredibly versatile with carrier and polymer type being only the first basic choices in design that must be followed up with consideration of specific polymer makeup, as well as carrier conformation, size, shape, and surface modifications. The design process can be very complicated especially as choices must be made in the scope of both biocompatibility and CA performance. With the meticulous integration of thoughtfully chosen polymers into a NP CA system, it is, however, possible to achieve lower cytotoxicity paired with better performance as compared to what is commercially available today.

Gadolinium-Based Nanoparticles. Instead of developing a completely novel CA formulation, one strategy is to improve upon the already-established use of Gd through polymerenhanced nanotechnology. The incorporation of Gd with biocompatible polymers could improve the toxicity profile of Gd CAs by limiting their release or minimizing direct contact between Gd ions and tissue. In addition, the barrier to clinical translation is low given that the CA basis, Gd, already has clinical approval and physicians already have experience with reading Gd-enhanced images. For this reason, many studies have examined commercially available GBCAs within their NP designs. 67-72 In addition to significant safety improvements, a NP system could create greater tunability for functionality and imaging properties and even allow for multimodal imaging applications.⁶ Although proof of noninferiority in imaging quality could be sufficient to push Gd-based NP systems to clinical realization when paired with better biocompatibility, some studies have also shown greater relaxivity values or contrast enhancement in imaging. Gd-based NP CA systems investigated since 2017 are outlined in Table 2.

AGuIX NPs are composed of a polysiloxane shell encapsulating an inorganic matrix covalently bound to clinically approved Gd-DOTA chelates. Phase I clinical trials AGuIX recently yielded promising results as combined therapeutic and

diagnostic tools for four types of brain metastasis. The NPs showed negligible toxicity at the maximum examined dosage of 100 mg/kg and had r_1 values greater than double that of unmodified Gd-DOTA, confirmed by enhanced brightness in T_1 -weighted images. Additionally, AGuIX NPs act as radiosensitizers, increasing the effectiveness of radiotherapy by enhancing radio wave targeting and magnifying its local strength. Phase II clinical trials began in 2019 and should be completed in 2023. 74

Recent research on Gd-based NPs focuses heavily on brain cancer due to the demand for better, earlier diagnostics and treatment. Effective MRI of brain tumors is essential for reliable diagnosis and could improve surgical outcomes by more clearly differentiating tumor edges to ensure complete removal. In a study aimed at glioma imaging, Patil et al. examined the effects of structural variation of NP CAs made up of Gd-DOTA bound to polymalic acid via PEG linkers arranged in a star shape. In all systems, glioma accumulation resulted, and high r_1 values were achieved. Many of the Gd-based NP CA systems under investigation in recent years take even more advanced approaches around brain cancer, aiming to add other functionalities on top of those necessary for enhancing MRI.

The growing field of theranostics, which combines therapeutics and diagnostics into a single system, is also well-represented within Gd-based CA research, such as the previously discussed AGuIX NPs. Another study combining the imaging and radiosensitization capabilities of Gd was performed by Shen et al. for orthotopic glioblastomas. Gd oxide NPs stabilized by poly(acrylic acid) (PAA), conjugated with lactoferrin and RGD dimers for tumor targeting, accumulated in glioblastoma tumors and resulted in an over 400% increase in contrast enhancement to MR images. Radiosensitization studies performed *in vitro* suggest that the NPs are both biocompatible and suitable as a radiosensitizer, further supported by increased survival time *in vivo*. 75

Multimodal imaging systems have also been investigated using Gd-based NPs. Multimodal imaging nanotechnology can be used for more than one imaging modality, such as computed tomography (CT), positron emission tomography (PET), or fluorescent imaging, to increase disease investigation and diagnosis accuracy by expanding upon available information.⁶ Therefore, the low sensitivity of MRI can be compensated for by gathering complementary information best suited to the strengths of each different imaging mode. Clinically approved Gd-DTPA was applied in a carbon nanodot (NCD) system coated with polymerized 1-methyl-2-pyrrolidinone (NMP) to image glioma in a multimodal application combining MRI and fluorescent imaging. This system showed lower toxicity and had an r_1 value 2.2 times greater than that of the commercially available Gd-DPTA, potentially explained by increased interaction with water due to the hydrophilicity of the polymer coating. When combined with the fluorescent functionality, high spatial resolution, and sensitivity were achieved in this synergistic approach.⁷⁶

While these systems have shown improved biocompatibility compared to commercially available GBCAs, the toxicity concerns around using exogenous metallic agents remain. For systems requiring brain localization, safety concerns are accentuated by the discovery of Gd deposition in the brain following GBCA use; concerns for NSF in those with impaired renal function remain, too. Gd-based agents also tend to have a short blood half-life, which may require repeated administration in order to generate desired images which also heightens the risk

Table 2. Summary of Polymeric Gadolinium-Based T_1 Contrast Agents

•	•			•					
Drug System	Target Condition	Admin.	Gd Agent	System Diameter	Polymer	Targeting moieties	$r_1 \; (\text{mM}^{-1} \; \text{s}^{-1}, \text{ magnetic field} $ strength)	Study Type	Ref
Thera-ANG-cHANPs	Glioma		Gd-DTPA	362 nm	Hyaluronic acid	Angiopep-2	8.86 (1.0 T)	In vitro	78
RVG & IRDye800- Gd,O,TNs	Neuroblastoma	vi	$\mathrm{Gd}_2\mathrm{O}_3$	37.5-42.5 nm	PEG	RVG peptide	9.901 (1.0 T)	In vivo (mouse)	42
ACh-MRNS	Acetylcholine in the brain	ic ^a	Gd(NP-DO3A)	96 nm	DSPE-PEG	BuChE	6.36 (7.0 T)	In vivo (rat)	80
pH-MRNs	Acetylcholine in the brain	ic	Gd(NP-DO3A)	77 nm	DSPE-PEG		6.91 (7.0 T)	In vivo (rat)	80
Gd3N@C80-loaded	Glioblastoma		Endofullerene	139-149 nm	PEG & DSPE-PEG	Transferrin, lactoferrin		In vitro	81
AIE-Gd dots	Whole brain	ÿ		38.9 nm	DSPE-PEG			In vivo (mouse)	82
NCDDG	Glioma	vi	Gd-DTPA		DTPA		8.06 (3.0 T)	In vivo (mouse)	71
$Poly(Gd(MAA)_3)$	Brain lesions and tumors		$Gd(MAA)_3$	40 nm	Polymethacrylic acid		12.613 (3.0 T)	In vitro	83
$\mathrm{Gd} \varnothing \mathrm{C}^{82}$ -Ala-PEG-Df- $^{89}\mathrm{Zr}$	Glioblastoma	vi	Gadofullerene	200 nm	PEG	cRGD		In vivo (mouse)	84
Gd ³⁺ -ALGD G2-asparagine	General brain and brain tu- mors	·Σ	$ ext{Cl}_3 ext{GdH}_{12} ext{O}_6$	254.1	PEG	Asparagine		In vivo (mouse)	88
AGuIX NPs	Brain metastasis	vi	Gd-DOTA		Polysiloxane		8.9 (3.0 T)	In vivo (human)	73
Gd-HP-AuNPs	Glioma	iv	$\text{Cl}_3\text{GdH}_{12}\text{O}_6$	75 nm	Heparin		9.89 (1.0 T)	In vivo (mouse)	98
AGuIX NPs	Glioma	vi	AGuIX	3 nm	Polysiloxane		6 (7.0 T)	In vivo (rat)	87
D-P(CPTM-co-DEA)-b-P (OEGMA-co-Gd-co- ANG)	Glioma	Ν	Gd-DOTA	75 nm	Camptothecin, DEA, oligo-(polyethylene glycol) monomethyl ether methacrylate	Angiopep-2	13.9 (3.0 T)	In vivo (rat)	88
PEG-Ce6-Gd NPs	Glioma	vi	$Gd(AC)_3$	120 nm	PEG		$0.43 \text{ mg/mL}^{-1} \text{ s}^{-1} (3.0 \text{ T})$	In vivo (mouse)	68
Col-Gd@Tub NC	Glioma	Ν	GdCl ₃	45 nm	Tubulin			In vivo (mouse)	06
MnGdOP@PDA-PEG	Brain tumor de- tection	subcu ^b	Gd oleate	1.8 nm	Polydopamine, PEG		6.7 (0.5 T)	In vivo (mouse)	91
AGuIX@PS @KDKPPR	Glioblastoma	vi	AGuIX	11.6	Polysiloxane	KDKPPR peptide	18.7 (1.4 T)	In vivo (mouse)	92
Eu-Gd (50-50%) NPs	Traumatic Brain Injury	vi	$\mathrm{GdCl}_{3}.x\mathrm{H}_{2}\mathrm{O}$	13.5 nm	PEG		4.77 (9.4 T)	In vivo (mouse)	93
Gd[DTPA]-loaded LTP NPs	Microglial cells		Gd-DTPA	269.2 nm	Poly(lactic-co-glycolic) acid, 1-tyrosinepolyphosphat	Triphenyl phosphonium, N-acetyl cysteine		In vitro	72
ES-GON-rBSA3-LF-RGD	Orthotopic Glio- blastoma	vi	$Gd(NO_3)_3$	13.4 nm	Polyactylic acid	RGD dimer, lactoferrin	15.1 (7.0 T)	In vivo (mouse)	75
GdF_3 NPs	Alzheimer's dis- ease		GdF_3	35 nm	PEG	Luminescent conjugated oligomers	0.40-0.55 (7.0 T)	In vivo (mouse)	94
Fn-Rev-Ang-GdDTPA	Glioma	vi	Gd-DTPA	6.8-1000 nm	Poly(amidoamine) dendrimers, DTPA	Angiopep-2, HREV-10	4.93 (3.0 T)	In vivo (mouse)	20
Gd-DDOTA-TPBP	Brain angiogra- phy and tu- mors	vi	Gd-DOTA	20 nm	Poly(ethylene glycol) methyl ether methacrylate (OEGMA), N-(2-hydroxypropyl) methacrylamide (HPMA)		7.19 (3.0 T)	In vivo (mouse)	98

Table 2. continued

 i ic: intracranial. b Subcu: subcutaneous.

,	Biom	ateria
	Ref	96
	Study Type	In vitro
	$r_1 \text{ (mM}^{-1} \text{ s}^{-1}, \text{ magnetic field strength)}$	4.8 (1.5 T)
	Targeting moieties	S-aminolevulinic acid, pentasodium tripoly- phosphate
	Polymer	
		Chitosan
	System Diameter	138 nm
	Admin. Gd Agent	$\mathrm{Gd}_2\mathrm{O}_3$
	Admin.	
	Target Condition	Glioblastoma
	Drug System	Gd2O3/CS-TPP@5-ALA NPs

of adverse effects.⁷⁷ For these reasons, alternate approaches in recent research predominantly use endogenous metals.

Iron-Based Nanoparticles. Iron-based NPs have consistently generated interest as a means of improving MRI because of their biocompatibility and magnetic properties. As iron (Fe) is naturally present in the body and can be degraded by natural mechanisms, it presents as a safe and more biocompatible alternative to GBCAs. The release of iron due to possible degradation of the NPs is mostly nontoxic at dosage levels needed for imaging application; most of the released iron seems to integrate into ongoing processes and metabolize in hemoglobin in the blood. Further supporting the development of Fe as a CA is its long blood half-life and flexible surface chemistry. The supporting the development of Fe as a CA is its long blood half-life and flexible surface chemistry.

Fe oxide NPs (IONPs) are the leading form of Fe-based imaging nanotechnology. Fe oxide generally refers to magnetite (Fe₃O₄) or the oxidized form, maghemite $(\gamma - \text{Fe}_2\text{O}_3)$. ¹⁰⁰ Coprecipitation from Fe²⁺ and Fe³⁺ ions is the most commonly used synthesis method for nanoparticles of either structure. 101 Alternative synthesis methods include microemulsions, laser pyrolysis, or thermal decomposition of other iron-containing species, such as iron acetyl acetonate. 100 Each preparation method aims to strictly control the size, shape, and magnetic properties of the iron oxide magnetic core. 102 Size has a significant impact on IONP MRI performance. IONPs with a size above 5 nm, termed superparamagnetic iron oxide nanoparticles (SPIONs), are suited for use in T_2 -weighted images where their accumulation causes a darkening of surrounding tissue. It has also been observed that larger SPIONs exhibit higher magnetization values and, therefore, offer greater contrast on MRI images, but the darkening effect is hard to interpret. 103 T₂ CA SPIONs continue to receive significant attention, but the clinical preference for T_1 -weighted CAs has shifted efforts toward systems designed for T_1 usage or with dual capabilities for T_1 - and T_2 -weighted imaging.

IONPs of a diameter less than 5 nm (often called ultrasmall superparamagnetic Fe oxide NPs or USPIONs) are advantageous for use in T_1 -weighted MRI. The small size of USPIONs allows for a greater surface area-to-volume ratio, which has been shown to increase r_1 which is essential for use as a T_1 CA. Additionally, the small magnetic moment of USPIONs suppresses the T_2 contrast effect. ¹⁸ A smaller size may also be advantageous for transport into through the BBB and renal clearance both known to be limited by size. Despite advantages of USPIONs, concerns have been raised around their toxicity. In a murine study comparing SPIONs and USPIONs, SPIONs of 9.3 nm exhibited no apparent toxicity, while USPIONs of 2.3 and 4.2 nm were highly toxic, as attributed to the induction of reactive oxygen species (ROS). 105 Still, some studies reviewed elsewhere cite excellent biocompatibility⁷¹ while others suggest that the biocompatibility of USPIONS depends on the quality of their coating. 106 Other methods for suppressing magnetization in order to reduce r_2 and allow r_1 to dominate include manipulations of shape, composition, and degree of crystallinity. Surface coating and doping can also enhance r_1 . Since CAs of this type generally result in more readable images than T₂-enhanced images and will resemble the contrast-enhanced images that physicians are already accustomed to seeing, clinical translation will be an easier transition for clinicians. Accordingly, T_1 Fe-based CAs have grown as the subject of much research now that routes for rendering longitudinal relaxivity their dominant magnetic factor have been established and explored.

Table 4. Summary of Polymeric Iron-Based T_1 Contrast Agents

		•)					
Drug System	Target Condition	Admin.	Core Diameter	System Diameter	Polymer	Targeting moieties	$r \left({_1 \text{ mM}^{-1} \text{ s}^{-1}, \text{ magnetic} \atop \text{field strength}} \right)$	Study Type	Ref
Fe-NCP	Brain tumor	Ϊ		97 nm	4-Bis (imidazole-1-ylmethil)-benzene; 3,4-dihydroxycinnamic acid		5.3 (r_1) , 10.9 (r_2) (7.0 T)	In vivo (mouse)	112
PA-USPIONs	Epileptic regions	vi	3.63 nm	13.7 nm	Maleimide (polyethyl-eneglyco	Pepstatin-A	4.16 (3.0 T)	In vivo (mouse)	110
ESIOs	Brain anatomy, stem cell tracing	ic	2.83 nm	3.43 nm	polyglucose sorbitol carboxymethyl ether		3.93 (7.0 T)	In vivo (rat)	122
SNIOs	Brain anatomy	ic	1.0 nm	3.1 nm	zwitterionic dopamine sulfonate		4.9 (7.0 T)	In vivo (mouse)	109
uIONP	Orthotopic glioblastoma	ic	3 nm	5.5 nm	Oligosaccharide (polymerized glucose)		$4.8 (r_1), 14.1 (r_2) (3.0 T)$	In vivo (mouse)	123
SPIO@DSPE-PEG/ DOX/ICG NPs	Glioma	iv		22.9 nm	1,2-Distearoyl-sn-glycero-3- phosphoethanolamine-N-methoxy(PEG)			In vivo (rat)	124
$\mathrm{Zn_{0.4}Fe_{2.6}O_4 ext{-}PEG ext{-}}$ RGERPPRs NPs	Glioma	iv	52 nm	110.7 nm	Polyethyle glycol	(RGERPPR)	47.4 (0.5 T)	In vivo (rat)	120
RGD-uIONPne/SN38	Glioblastoma	iv	3.5 nm	12.4 nm	Poly(ethylene glycol)-block-allyl glycidyl ether	cyclo (Arg-Gly-Asp-D-Phe-Cys		In vivo (mouse)	125
SIONs@ANG/Ce6/PE	Brain disease diagnostics	iv	4.5 nm	24.3 nm	PEG	Angiopep-2	$21.2 \ (r_1), 93.2 \ (r_2) \ (0.5 \ \mathrm{T})$	In vivo (mouse)	126
NG/PEG-USPIONs	Glioblastoma	iv	3.5 nm	14.60 nm	PEG	Angiopep-2	4.68 (3.0 T)	In vivo (mouse)	18
T7-CD-CS-polyGIO NPs	Orthotopic glioma	in ^a	34 nm	53.1 nm	eta-Cyclodextrin-chitosan; PEG	T7 peptide		In vivo (mouse)	1111
ESIONPs	Whole brain	ic	3 nm	11 nm	PEG			In vivo (mouse)	17
QA-USIONPs	Brain cancers		3.0 nm	38 nm	Quinic acid		1.1 (r_1) , 6.3 (r_2)	In vitro	28
nBCA	Brain cancers	vi	11111 C:-7	mu 99	PEG	Catechol	3.951 (7.0 T)	In vivo	16
HS-COOH	Brain anatomy	iv	24.2 nm	43.4 nm	Carboxylic acid		320 (6.5 mT)	In vivo	127
HS-PEG	Brain anatomy	iv	24.2 nm	92.9 nm	PEG		261 (6.5 mT)	In vivo (rat)	127
${ m Fe_3O_4} ext{-ANG NPs}$	Glioblastoma	ÿ	3.3 nm	~25 nm	PEG	Angiopep-2	7.46 (3.0 T)	In vivo (mouse)	128
$\mathrm{CNC\text{-}PCA/Fe}_3\mathrm{O}_4$	General brain		13.2 nm	12.0 nm	Cellulose nanocrystals-poly(citric acid)		13.8 (3.0 T)	In vitro	129
nIBCA	Brain tumor	Ϋ́	168 Da	4200 Da	PEG	3,4-dihydroxyhydrocinnamic acid, nordihydroguaiaretic acid	3.951 (7.0 T)	In vivo (mouse)	130
EM	Epilepsy	vi		95 nm	PEG-PLA-ferrocene	Angiopep-2	5.9 (7.0 T)	In vivo (mouse)	131
Nanoclusters	Brain drug delivery	ÿ	4 nm	200 nm	Tannic acid	Bovine serum albumin	4.78 (9.4 T)	In vivo (mouse)	132
SAIO	General brain and brain vessels		3 nm	5, 9, 12 nm	Dextran		3.8 (1.5 T)	In vivo (rat)	133
^a in: intranasal.									

Most studies focus on spherical IONPs, but other morphologies are possible through different synthesis strategies and conditions. Roca et al. note that IONP shape and size can impact both the magnetic properties and other biomedically relevant properties, such as colloid ability, cellular uptake, and toxicity. ¹⁰⁷

While a few IONP formulations have received FDA approval, none have been approved for neurologic applications and most have not remained on the market; in addition, most of them function as T_2 CAs. 100,102,108 However, various formulations have shown early promise for brightening enhancements to T_1 weighted MR images of the brain. One study utilized single nanometer iron oxide NPs (SNIOs) coated with zwitterionic dopamine sulfonate. The small size of the NPs increased brain permeability and enabled whole-brain visualization on MRI. The SNIOs were designed at a size comparable to Gd-DPTA, smaller than most IONPs reported, and yet the per-particle r_1 values were approximately 13 times higher than that of Gd-DPTA under the same magnetic field strength. 109 Du et al. designed ultrasmall PEGylated SPIONs, with a Fe₃O₄ core diameter of 3.63 ± 0.41 nm, to visualize epileptic regions of the brain using pepstatin-A, which targets proteins overexpressed with epilepsy. Use as a T_1 CA was supported by a high r_1 value of 4.16 mM⁻¹ s⁻¹, comparable to commercially available Gd-DPTA, paired with highly efficient epileptogenic region targeting as verified by Prussian blue staining. 110

The majority of Fe-based T_1 neurological CA systems have been designed to target brain cancers. Angiopep-2 was used to effectively target PEGylated IONPs with a uniform metallic core of 3.5 nm into intracranial glioblastoma in a murine model. The brightening effect observed on T_1 -weighted MR images was shown to be concentration-dependent; the maximum concentration of IONPs within tumors occurred at 2 h, after which signal brightening was maintained for another 4 h. The r_1 was as high as 4.68 mM⁻¹ s⁻¹, outperforming commercially available Gd-DPTA. 18 Many brain cancer targeting systems are also multifunctional with theranostic or multimodal approaches. Sukumar et al. synthesized a theranostic, multimodal system for imaging orthotopic glioblastoma based on gold-iron oxide NPs (GIONs). GIONs were first coated with β -cyclodextrinchitosan onto which T7-peptide was conjugated via PEG linkers for tumor targeting. The NPs were loaded with tumorsuppressing miRNAs and the chemotherapeutic drug Temozolomide. Dye labeling to the miRNAs allowed in vivo fluorescent imaging to be used in conjunction with MRI. Ultimately, selective accumulation into brain tumors was observed via both imaging modalities, and treatment efficacy was supported by prolonged survival time and positive health indicators for treated versus control mice.111

Fe-based CAs have generated interest as dual T_1/T_2 CAs because of the metal's capacity to enhance T_1 - or T_2 -weighted images depending on the design. Dual CAs aim to reduce T_1 and T_2 simultaneously; they aim to overcome shortcomings of each individual CA type by generating complementary information. A unique advantage of dual CAs is easy cross-validation because dual systems can be used in the same MRI scanner, allowing the images to be spatially and temporally matched. In a study comparing nanoscale coordination polymers (NCP) containing different metals (Fe³⁺, Gd²⁺, Mn²⁺) for feasibility as dual CAs in brain tumors, it was seen that only the Fe-NCP form showed promise as a dual T_1/T_2 CA. Relaxivity values of 5.3 mM⁻¹ s⁻¹ and 10.9 mM⁻¹ s⁻¹ were achieved for r_1 and r_2 , respectively, and

tumoral accumulation was observed within a matter of minutes after intravenous administration. 112

Other Fe-based nanotechnology includes metal alloys and metal doped IONPs. Metal alloys that have been the subject of imaging research are often bimetallic; some of those include gold–Fe, nickel–Fe, and Gd–Fe NPs. 113 Metals used for doping IONPs include zinc, 114 copper, 115 gadolinium, 116,117 and manganese. 118 One major strength of these systems is that the combination of magnetic properties could result in a greater influence on relaxation time; for this reason, the relaxivity achieved by multimetal contrast agents is significantly higher than what can be achieved by IONPs alone. 103 In addition, the combination of differing magnetic and metallic properties can increase the potential for multifunctionality. 119 Chen et al. designed a liposome-coated, zinc-doped IONP system functionalized with PEG and tumor-penetrating peptide (RGERPPR) for glioma targeting. The zinc doping increased the magnetic saturation strength of the IONP, resulting in a high r_1 of 47.4 mM^{-1} s⁻¹ at 0.5 T, supporting its use as a T_1 contrast agent. Furthermore, image enhancement was observed with a 7.29% signal increase in tumor cells upon that of the control. 120

Table 4 presents an inclusive list of Fe-based systems recently explored for use within the brain. Despite increased relaxivity and functionality in combined metal systems, the inclusion of non-native metals in the body significantly affects biocompatibility. Further research is necessary to address toxicity concerns before the development of these bimetallic CAs can be widely pursued. For this reason, these systems are much more limited in literature than that of IONP systems. IONPs, however, have been noted to be biocompatible in most studies.

The predominant limitation of Fe-based T_1 CAs to date is that the magnetic properties of Fe tend to serve best as T2 CAs, meaning that system design is further complicated to allow longitudinal relaxation to become the dominant factor in MRI enhancement. Therefore, the financial incentives for development are lacking as the costs of production for complicated or time-consuming synthesis processes may outweigh the potential for profit." Although toxicity is generally low in Fe-based systems, biocompatibility concerns associated with ultrasmall designs may limit some of the feasible strategies for augmenting relaxivity. For USPIOs or IONPs with complex morphologies, toxicity and stability concerns arise due to the high surface energies of systems with such large surface area to volume ratios which may make them prone to aggregation and oxidation.⁷ Oxidation can cause DNA damage and induce cellular cascades that can lead to an array of adverse effects. 121 To that point, the addition of antioxidants or iron chelators can protect against oxidative stress.

Manganese Based Nanoparticles. Manganese-based contrast systems are of particular interest for MRI application due to the paramagnetic properties of its divalent ions. Like Gd-based systems, these systems tend to be most suited to enhancing T_1 -weighted images, with a brightening effect observed in response to accumulated manganese (Mn) ions. Mn-based NP systems are more biocompatible than the gold standard, Gd, since manganese is naturally found in the body. $^{134-136}$ Additionally, Mn can cross the BBB since it serves as a cofactor for various receptors and enzymes. 136

Early approaches 137 for Mn-based CAs took the form of either free Mn, administered in an ionic form, or chelated Mn. Lumenhance, a free ion form of magnesium chloride $(MnCl_2)$, 138 and Teslascan, a dipyridoxyl diphosphate chelated form of Mn, 139 both received FDA approval as MRI CAs for use

Table 5. Summary of Polymeric Manganese-Based T_1 Contrast Agents

Drug System	Target Condition	Admin.	Core Admin. Diameter	System Diameter	Polymer	Targeting Moieties	Relaxivity (mM^{-1} s ⁻¹ , magnetic field strength)	Study Type	Ref
Hollow Mn ₃ O ₄	Brain anatomy	ic	24.3 nm	varies	PEG, phospholipids	Carboxylate, alcohol, thiol, amine	0-1.40 (3.0 T)	In vivo (mouse)	151
iRPPA@TMZ/MnO	Glioma	ïv	15 nm	71 nm	Polyethylene glycol-poly(2- (diisopropylamino)ethyl methacrylate	Internalizing arginine- glycine-aspartic acid	42.21 (3.0 T)	In vivo (rat)	152
Ultrasmall MnO	Brain cancer	ÿ	2.7 nm	22.2	Polyacrylic acid	Folic acid	9.3 (3.0 T)	In vivo (mouse)	153
ANG-MnEMNPs-Cur, AMEC	Traumatic brain injury	ïv	160 nm	200 nm	Eumelanin	Angiopep-2	4.5 (7.0 T)	In vivo (mouse)	150
Nanogel-based neural interface with captured Mn ²⁺	Functional brain anatomy			50-200 nm	Chitosan-modified poly(3,4 -ethylenedioxythiophene)		0.00598 (7.0 T)	In vitro	154
tLyP-1-CD-DOPA-MnO2@ PTX	Orthotopic glioma	ÿ	14.2 nm	159.8 nm	Dopamine- eta -cyclodextrin	tLyP-1	6.02 (3.0 T)	In vivo (rat)	135
HA-MnO2 NPs	Glioma	ic	7 nm	83 nm	Hyaluronic acid		13.93 (3.0 T)	In vivo (rat)	61
MnO@PMA NPs	Neurological conditions and brain cancer		15.9 nm	17.7 nm	Poly(isobutylene-alt-maleic anhydride)		7.7 (7.0 T)	In vitro	155
MnO@PLGA NPs	Neurological conditions and brain cancer		15.9 nm	163.0 nm	Poly(D,L-lactide-co-glycolide)		0.24 (7.0 T)	In vitro	155
Mn coordinated carbon quantum nanodots	General anatomy, brain included	ÿ		64.41 nm	Tannic acid		2.43 (0.5 T)	In vivo (mice)	156
aAβ-BTRA-NC MnO ₂ -NPs	Alzheimer's Disease	ÿ		68.6 nm	Poly(methacrylic acid), polysorbate 80	Anti-A eta antibody	16.7 (7.0T)	In vivo (mice)	157
Chitosan-Mangafodipir mNPs	Neuro-degenerative disease	. II	90–114 nm		Chitosan		Enhancement noted by %	In vivo (mice)	158
Mn-NCP	Brain tumors	iv		121 nm	4-Bis (imidazole-1-ylmethil)-benzene; 3,4-dihydroxycinnamic acid		3.7 (7.0 T)	In vivo (mice)	112

in the abdomen and pelvis in 1997. Both drugs only remained on the market for a few years before being discontinued over toxicity concerns around Mn ion accumulation; for Mn-based CAs to be realized clinically, a shift in approach became necessary. Manganese oxide nanoparticles (MONs), which exhibit negligible toxicity under limited concentrations and can be cleared from the body via renal filtration, emerged as a promising option. ¹⁴⁰, ¹⁴¹ Most commonly, MONs are synthesized by thermal decomposition of manganese-containing compounds such as manganese oleate or manganese acetate. ¹⁴²

Size, shape, and composition significantly impact the magnetic properties of MONs. Greater surface area has been shown to result in greater r_1 values ^{143,144} because the Mn²⁺ ions interact with surrounding tissue most directly at the surface of the NP. Smaller particles are, therefore, often considered desirable as they have a greater surface area-to-volume ratio. MONs is versatile in terms of composition since Mn has a wide range of oxidation states. It has been observed that the paramagnetic payload of MONs is maximized at lower valence states of manganese, making MnO (oxidation state: + 2) very appealing, with Mn_3O_4 (oxidation state: mix of +2 and +3) not far behind. 145 One study showed that faster temperature ramping paired with shorter aging times for the decomposition reaction produced the smallest MONs, but the selectivity for the desired MON composition suffered under these conditions. 146 Therefore, optimization for synthesis parameters is necessary to achieve the desired balance of composition and size.

A special category of MONs that do not generate MRI contrast under standard biological conditions has emerged in recent years. MONs composed of higher valence state Mn allow for contrast effects to be activated by the environment itself. In Mn-based systems, the $\mathrm{Mn^{2+}}$ ion is predominantly responsible for altering relaxation time. ¹⁴⁷ MRI contrast in a higher valence MON system is generated by the reduction and release of the manganese oxide to expose the more strongly paramagnetic Mn²⁺ components at the surface of the NP. The reduction to the Mn²⁺ state has been shown to be triggered by acidic pH and redox agents such as H₂O₂ and glutathione. ¹⁴⁸ The result is that under acidic or otherwise reductive conditions, Mn²⁺ ions are released from MONs, turning the contrast "ON" and activating the image enhancement in areas containing the paramagnetic species. The activatable nature of environmentally responsive MONs offers benefits to static systems such as refined sensitivity and specificity. 135 Responsive MON systems are typically designed with MnO2, which is highly reactive compared to other compositions.

The release-triggering conditions for reductive MONs have been found to be particularly useful in the case of brain tumors as tumor environments have been shown to be acidic and concentrated in reducing agents. 148 Making responsive MONs even more appealing is their ability to combat hypoxia, as a direct result of the reaction with the tumor microenvironment. The reduction of MnO₂ not only activates image enhancements by releasing Mn²⁺ but also produces oxygen and reactive oxygen species (ROS). 135 The oxygen production directly reduces hypoxia, allowing for increased efficacy for treatments like chemotherapy or radiotherapy, while the ROS are cytotoxic to the tumor, inhibiting its growth. Although ROS generation can be desirable when controlled and applied as a treatment, oxidative stress resulting from MON reduction can harm healthy tissue, causing DNA damage or apoptosis. 140 Addressing these concerns, it has been shown that MONs can also act as ROSscavengers, with MnO₂ having the most scavenging potential.

Therefore, a balance of pro- and antioxidation activity must be accounted for in design considerations to minimize toxicity. 149

Jiang et al. also relieved hypoxia in glioma in using $\rm H_2O_2$ -reactive theranostics. The system was coloaded with paclitaxel, a chemotherapeutic drug, and $\rm MnO_2$; both active agents were released upon the degradative, oxygen-producing reaction of $\rm MnO_2$ in the tumor. Relaxivity increased from 3.30 mM $^{-1}$ s $^{-1}$ to 6.02 mM $^{-1}$ s $^{-1}$ at a field strength of 3.0 T when tested under standard acid or $\rm H_2O_2$ -containing conditions, respectively, which was reflected by increased signal intensities of intracranial glioma in mice on T_1 -weighted images. The therapeutic efficacy was confirmed as treated mice experienced increased survival time and a gradual decrease in tumor size, which was attributed to the synergistic treatment effects of paclitaxel and $\rm MnO_2$.

Manganese in forms other than manganese oxide has been investigated but is less documented to date. Nanocomposite structures made up of manganese-doped eumelanin, a natural polymer, and loaded with curcumin, a neuroprotective agent, were designed with antineuroinflammatory functionalities and diagnostic MRI capabilities for traumatic brain injuries (TBI). The theranostic was targeted to traumatized brain tissue using Angiopep-2. Eumelanin and curcumin served therapeutic purposes primarily, working to alleviate oxidative stress, promote neuro-regeneration, and relieve neuroinflammation. Magnesium doping rendered the system effective as a dual T_1 – T_2 CA for the visual tracking of drug delivery into TBI lesions, as evidenced by high r_1 and r_2 values of 4.5 and 53.7 mM $^{-1}$ s $^{-1}$ at 7.0 T, respectively. 150

Table 5 provides an overview of Mn-based, polymeric approaches for imaging the brain or disease conditions of the brain.

The primary factor limiting the widespread clinical application of Mn-based systems is that the relaxivity values achieved are generally considered insufficient compared to the current gold standard. Many MONs have lower relaxivities than that of FDA-approved systems, making clinical translation tricky. Although the biocompatibility of Mn may be greater than Gd, it can still have toxic effects in high amounts-namely, it can trigger a neurodegenerative disorder termed "manganism". 136 Mn²⁺ ions can be also erroneously recognized as Ca²⁺ ions, which could disturb the regulation and function of many bodily processes. 137 Mn's stability is lower than Gd's. Transmetalation with endogenous metals like copper, calcium, and zinc can all trigger Mn ion release to cause the aforementioned effects; 136 system design and polymer modifications should aim to curb this. Nonetheless, if high relaxivity was achieved and toxicity concerns addressed, MONs could be a highly desirable option given the greater ease for generating T_1 contrast enhancement as compared to Fe-based systems and greater biocompatibility as compared to Gd-based systems.

Future Directions. Nanomedicine is the emerging option for diagnostics of CNS disorders due to the unique properties and tunability of NPs. The future of CAs relies heavily on the continued improvements in nanotechnology and therefore will need to be pursued as a coordinated effort involving engineers, materials scientists, medical researchers, and clinicians. ¹²¹ Gd, Fe, and Mn each still present their own set of toxicity concerns, and addressing these has to be at the forefront of design if clinical translation is to be achieved. Polymers present as an option to mask the metal from direct contact with tissue, without eliminating the necessary water contact, in order to address any concerns from direct contact. Additionally, polymeric encapsulation of the metals and/or metal ions can increase

control over delivery rates, while still allowing the CA to remain in the body long enough to capture multiple or real-time images. In general, the addition of a polymer to a metal-based CA system can enhance stability of these metal ions by increasing circulation time and controlling metal release rates. Ultimately, the specific application will drive polymer choice to address tissue-based or route of administration-based concerns.

A farther-reaching impact, however, is the potential to achieve higher relaxivity values than any system that has thus far made it to the clinical realm. Clinically available CAs function based purely on the magnetic properties of the metal itself. By adding polymers, those same properties will be in play but magnified by the additional benefits of the polymer; the polymers will primarily increase the interaction between water and the metal beyond what occurs naturally, which increases relaxivity. This means the brightening effect observed on a contrast-enhanced MR image will be more extreme, increasing the confidence of diagnosis by making tissue differences more obvious and images easier to read. This will be a major stride for diagnostics in general but is especially exciting in application with CNS disorders, for which contrast enhanced MRI has only been clinically available for a select few diseases due to difficulty in CA delivery. 21,159

The capacity of polymers to improve both biocompatibility and enhance contrast of magnetic metals is something that will prove incredibly important in the development of clinically translatable CAs. Metals like Mn and Fe tend to fail the superiority test when comparing to GBCAs based on MRI performance parameters—either the strength or mode of enhancement—though their cytotoxicity is better. By exploiting the tunable properties of polymers and maximizing CA contact with the water content of surrounding tissues, CA performance can be altered to magnify their already extant magnetic properties and turn them into high-strength T_1 MRI enhancers. Because of this, Mn and Fe could become clinically translatable when placed in a polymeric delivery system, maintaining the low cytotoxicity of these metals, while simultaneously improving contrast and stability due to the presence of the polymer. The addition of polymers can also improve already existing GBCAs; by masking GBCAs in larger polymeric delivery systems, this could decrease interactions with the kidney filtration system based on size alone 160 and decrease the negative effects of GBCAs on patients with renal impairment.

Other techniques for tuning relaxivity will continue to focus on the development of the metal itself. The fine-tuning of different synthesis can allow for augmentation of size and shape as well as other factors that affect r_1 like metal composition. 100,145 For example, although most CA publications cite a specific metal composition for their CA, many are mixtures of various compositions. For example, both magnetite and maghemite appear in IONPs but maghemite is preferable for T_1 usage due to its greater number of unpaired electrons;⁷⁷ similar r_1 preferences exist for MON compositions. Thus, controlling the extent of metal oxidation to achieve a favorable compositional ratio through parameters like temperature, solvent, and reaction extent is a widely relevant technique for influencing r_1 . Further exploration of multiple-metal CAs also has potential to improve image-enhancing capabilities, although the inclusion of additional metals will only add more toxicity considerations.⁷⁷ Any improvements made on the metals used as CAs can be incorporated into polymer delivery systems, thus enhancing the improvements.

Brain targeting is another point that requires improvement when designing brain-specific CAs. The brain has long remained poorly understood and under-treated on account of the BBB. However, recent advances in targeting mechanisms and increasing knowledge on brain transport open new doors for many brain-aimed drugs, 1-3,50 including CAs. Techniques for improving brain transport include surface coating and ligand bioconjugation. Suitable targeting motifs (natural and synthetic alike) are continuing to be investigated; the combination of multiple targeting moieties to a single CA may further improve brain targeting while also eliminating off-target effects of the CAs by increasing the likelihood of contact with an appropriate receptor. 121 The addition of polymers to CAs will allow for increased bioconjugation functionality without disrupting any beneficial properties of the metal. Brain-targeting ligands $^{1-3,50,161}$ like apolipoprotein E, $^{162-164}$ apolipoprotein B, $^{165-167}$ transferrin, $^{168-171}$ and insulin $^{172-174}$ have all been used to bypass the BBB in polymer-based delivery systems. Leveraging these advances using polymer-based systems to encapsulate and deliver CAs to the brain is a logical next step. Furthermore, dense PEG coatings themselves have been demonstrated to lead to increased brain penetration and could be taken advantage of to improve CA delivery to the brain. 175 Alternate administration routes, such as intranasal, can also be exploited to improve CA delivery both with and without polymers. 121 Because the brain is much more complicated for drug delivery than other organ systems, it follows that medical advancement in other parts of the body will precede similar applications in the brain. Therefore, it is also expected that functionalities that are being developed for application in other body systems, such as enzyme-activated CAs, 176 will also be integrated into brain-specific designs. Additionally, new animal models are being developed that model the pathogenesis of various CNS diseases as well as the human BBB more accurately than traditional mouse or rat models and these will prove to be integral for performance screening and in vivo evaluations leading up to preclinical trials. 121

Increasing attention has been paid to CAs with multiple or specialized functionalities. To simplify and personalize the treatment process with patients in mind, researchers are aiming to elevate CA design by tackling multiple tasks all within a single device as in theranostic and multimodal CAs. Multifunctional, theranostic, and dual-contrast CAs have the potential to not only streamline therapeutic management, allow for real-time disease tracking and individualized treatment plans, and improve diagnostics. 121 Some polymer systems, like polymersomes, can coencapsulate multiple therapeutic molecules, which eliminates the need for multifunctional CAs; instead, multiple therapeutic modalities could be coencapsulated in the polymer system to gain benefits of both. ^{177,178} Specialized applications are also being developed for neurological diseases that have not been previously compatible with imaging. CA targeting of disease biomarkers is attractive for diseases that do not exhibit obvious structural differences so novel CAs designed for use with specific diseases other than brain cancers are expected to see a rise in literature.

CONCLUSION

MRI of the brain relies heavily on the use of CAs, which enhance signal differences between tissues. New technology is necessary to replace the only commercially available contrast agents that present toxicity concerns and fail to cross the BBB under normal conditions. Polymeric nanotechnology approaches utilizing the

magnetic properties of gadolinium, iron, or manganese have sought to fill this need. The integration of nanomedicine and polymers into a contrast-enhancing agent allows for a combination of functionality and design strengths which yield improved biocompatibility and superior transport and disease targeting and most importantly, increased relaxivity and imageenhancing capabilities. While gadolinium-based agents are more established in clinical settings, options utilizing iron and manganese offer a greater biocompatibility potential. Various combinations of these magnetic metals and polymers have been explored for applications within the brain, with increased contrast enhancing performance compared to commercially available agents, as well as better biocompatibility being a common observance among polymeric CAs. With many of those systems having seen encouraging levels of success at various stages (in vitro, in vivo, and in clinical trials), the future of CAs for MRI shows great promise for more readable images and increased safety.

AUTHOR INFORMATION

Corresponding Authors

Dorian Foster — Department of Chemical and Biomolecular Engineering, Clemson University, Clemson, South Carolina 29631, United States; orcid.org/0000-0003-4452-1257; Email: dnfoste@clemson.edu

Jessica Larsen — Department of Chemical and Biomolecular Engineering and Department of Bioengineering, Clemson University, Clemson, South Carolina 29631, United States; orcid.org/0000-0003-2756-9523; Email: larsenj@clemson.edu

Complete contact information is available at: https://pubs.acs.org/10.1021/acsbiomaterials.2c01386

Notes

The authors declare no competing financial interest.

REFERENCES

- (1) Larsen, J. M.; Martin, D. R.; Byrne, M. E. Recent Advances in Delivery through the Blood-Brain Barrier. *Curr. Top Med. Chem.* **2014**, 14 (14), 1148–1160.
- (2) Pardridge, W. M. Blood-Brain Barrier Delivery. *Drug Discov Today* **2007**, *12* (1–2), 54–61.
- (3) Furtado, D.; Björnmalm, M.; Ayton, S.; Bush, A. I.; Kempe, K.; Caruso, F. Overcoming the Blood-Brain Barrier: The Role of Nanomaterials in Treating Neurological Diseases. *Adv. Mater.* **2018**, 30, 1801362.
- (4) Dong, X. Current Strategies for Brain Drug Delivery. *Theranostics*; Ivyspring International Publisher, 2018; pp 1481–1493, DOI: 10.7150/thno.2125.
- (5) MRI. CancerQuest. https://www.cancerquest.org/patients/detection-and-diagnosis/magnetic-resonance-imaging-mri (accessed 2022-08-30).
- (6) Wang, C.; Wang, X.; Chan, H. N.; Liu, G.; Wang, Z.; Li, H. W.; Wong, M. S. Amyloid- β Oligomer-Targeted Gadolinium-Based NIR/MR Dual-Modal Theranostic Nanoprobe for Alzheimer's Disease. *Adv. Funct Mater.* **2020**, *30* (16), 1909529.
- (7) Benefits and Risks. FDA. https://www.fda.gov/radiation-emitting-products/mri-magnetic-resonance-imaging/benefits-and-risks (accessed 2022-08-30).
- (8) Ionizing Radiation—Health Effects. Occupational Safety and Health Administration. https://www.osha.gov/ionizing-radiation/health-effects (accessed 2022-11-04).
- (9) Cai, X.; Zhu, Q.; Zeng, Y.; Zeng, Q.; Chen, X.; Zhan, Y. Manganese Oxide Nanoparticles as Mri Contrast Agents in Tumor

- Multimodal Imaging and Therapy. International Journal of Nano-medicine 2019, 8321–8344.
- (10) How Strong Does Your MRI Magnet Really Need to Be? *DMS Health*. https://www.dmshealth.com/05/how-strong-does-mrimagnet-need-to-be/ (accessed 2022-08-28).
- (11) Grover, V. P. B.; Tognarelli, J. M.; Crossey, M. M. E.; Cox, I. J.; Taylor-Robinson, S. D.; McPhail, M. J. W. Magnetic Resonance Imaging: Principles and Techniques: Lessons for Clinicians. *Journal of Clinical and Experimental Hepatology* **2015**, 246–255, DOI: 10.1016/j.jceh.2015.08.001.
- (12) Broadhouse, K. M. The Physics of MRI and How We Use It to Reveal the Mysteries of the Mind. *Front. Young Minds* **2019**, DOI: 10.3389/frym.2019.00023.
- (13) Zhang, Y.; Cheng, J.; Liu, W. Characterization and Relaxation Properties of a Series of Monodispersed Magnetic Nanoparticles. Sensors (Switzerland) 2019, 19 (15), 3396.
- (14) NMR: Relaxation and its characteristics: T1 and T2 times. https://www.imaios.com/en/e-Courses/e-MRI/NMR/Relaxation-nmr (accessed 2022-08-27).
- (15) MRI Basics. https://case.edu/med/neurology/NR/MRI%20Basics.htm (accessed 2022-08-27).
- (16) Xue, X.; Bo, R.; Qu, H.; Jia, B.; Xiao, W.; Yuan, Y.; Vapniarsky, N.; Lindstrom, A.; Wu, H.; Zhang, D.; Li, L.; Ricci, M.; Ma, Z.; Zhu, Z.; Lin, T.-y.; Louie, A. Y.; Li, Y. A Nephrotoxicity-Free, Iron-Based Contrast Agent for Magnetic Resonance Imaging of Tumors. *Biomaterials* **2020**, 257, 120234.
- (17) Kim, J. H.; Dodd, S.; Ye, F. Q.; Knutsen, A. K.; Nguyen, D.; Wu, H.; Su, S.; Mastrogiacomo, S.; Esparza, T. J.; Swenson, R. E.; Brody, D. L. Sensitive Detection of Extremely Small Iron Oxide Nanoparticles in Living Mice Using MP2RAGE with Advanced Image Co-Registration. *Sci. Rep* **2021**, DOI: 10.1038/s41598-020-80181-9.
- (18) Du, C.; Liu, X.; Hu, H.; Li, H.; Yu, L.; Geng, D.; Chen, Y.; Zhang, J. Dual-Targeting and Excretable Ultrasmall SPIONs for: T 1-Weighted Positive MR Imaging of Intracranial Glioblastoma Cells by Targeting the Lipoprotein Receptor-Related Protein. *J. Mater. Chem. B* **2020**, 8 (11), 2296–2306.
- (19) Lohrke, J.; Frenzel, T.; Endrikat, J.; Alves, F. C.; Grist, T. M.; Law, M.; Lee, J. M.; Leiner, T.; Li, K. C.; Nikolaou, K.; Prince, M. R.; Schild, H. H.; Weinreb, J. C.; Yoshikawa, K.; Pietsch, H. 25 Years of Contrast-Enhanced MRI: Developments, Current Challenges and Future Perspectives. *Advances in Therapy*. Springer Healthcare, January 1, 2016; pp 1–28. DOI: 10.1007/s12325-015-0275-.
- (20) Beyer, S.; Sebastian, N. T.; Prasad, R. N.; Chu, J.; Liu, K.; Madan, K.; Jiang, W.; Ghose, J.; Blakaj, D. M.; Palmer, J. D.; Eltobgy, M.; Otero, J.; Elder, J. B.; Raval, R. R. Malignant Ossifying Fibromyxoid Tumor of the Brain Treated with Post-Operative Fractionated Stereotactic Radiation Therapy: A Case Report and Literature Review. *Surg Neurol Int.* **2021**, *12*, 588.
- (21) Wahsner, J.; Gale, E. M.; Rodríguez-Rodríguez, A.; Caravan, P. Chemistry of MRI Contrast Agents: Current Challenges and New Frontiers. *Chemical Reviews* **2019**, 957–1057, DOI: 10.1021/acs.chemrev.8b00363.
- (22) Do, C.; DeAguero, J.; Brearley, A.; Trejo, X.; Howard, T.; Escobar, G. P.; Wagner, B. Gadolinium-Based Contrast Agent Use, Their Safety, and Practice Evolution. *Kidney360* **2020**, *1* (6), 561–568.
- (23) Wan, F.; Wang, L.; Xu, W.; Li, C.; Li, Y.; Zhang, C.; Jiang, L. Binuclear Gadolinium(III) Complex Based on DTPA and 1,3-Bis(4-Aminophenyl)Adamantane as a High-Relaxivity MRI Contrast Agent. *Polyhedron* **2018**, *145*, 141–146.
- (24) Bai, J.; Wang, J. T. W.; Rubio, N.; Protti, A.; Heidari, H.; Elgogary, R.; Southern, P.; Al-Jamal, W. T.; Sosabowski, J.; Shah, A. M.; Bals, S.; Pankhurst, Q. A.; Al-Jamal, K. T. Triple-Modal Imaging of Magnetically-Targeted Nanocapsules in Solid Tumours in Vivo. *Theranostics* **2016**, *6* (3), 342–356.
- (25) Serkova, N. J. Nanoparticle-Based Magnetic Resonance Imaging on Tumor-Associated Macrophages and Inflammation. *Frontiers in Immunology* **2017**, DOI: 10.3389/fimmu.2017.00590.
- (26) Werner, E. J.; Datta, A.; Jocher, C. J.; Raymond, K. N. High-Relaxivity MRI Contrast Agents: Where Coordination Chemistry

- Meets Medical Imaging. Angewandte Chemie International Edition 2008, 47, 8568-8580.
- (27) Strbak, O.; Balejcikova, L.; Kmetova, M.; Gombos, J.; Kovac, J.; Dobrota, D.; Kopcansky, P. Longitudinal and Transverse Relaxivity Analysis of Native Ferritin and Magnetoferritin at 7 T MRI. *Int. J. Mol. Sci.* **2021**, 22 (16), 8487.
- (28) Narkhede, A. A.; Sherwood, J. A.; Antone, A.; Coogan, K. R.; Bolding, M. S.; Deb, S.; Bao, Y.; Rao, S. S. Role of Surface Chemistry in Mediating the Uptake of Ultrasmall Iron Oxide Nanoparticles by Cancer Cells. ACS Appl. Mater. Interfaces 2019, 11 (19), 17157–17166.
- (29) Hagberg, G. E.; Scheffler, K. Effect of R1 and R2 Relaxivity of Gadolinium-Based Contrast Agents on the T1-Weighted MR Signal at Increasing Magnetic Field Strengths. *Contrast Media Mol. Imaging* **2013**, *8* (6), 456–465.
- (30) Tweedle, M. F.; Kanal, E.; Muller, R. Considerations in the Selection of a New Gadolinium-Based Contrast Agent. *The Journal of Practical Medical Imaging and Management* **2014**, No. Suppl, 1–11.
- (31) Kanal, E.; Maravilla, K.; Rowley, H. A. Gadolinium Contrast Agents for CNS Imaging: Current Concepts and Clinical Evidence. *American Journal of Neuroradiology*. American Society of Neuroradiology December 1, 2014; pp 2215–2226. DOI: 10.3174/ajnr.A3917.
- (32) Heshmatzadeh Behzadi, A.; McDonald, J. Gadolinium-Based Contrast Agents for Imaging of the Central Nervous System: A Multicenter European Prospective Study. *Medicine (United States)* **2022**, *101* (34), E30163.
- (33) Information on Gadolinium-Based Contrast Agents. FDA. https://www.fda.gov/drugs/postmarket-drug-safety-information-patients-and-providers/information-gadolinium-based-contrast-agents (accessed 2022-08-27).
- (34) Gadoterate meglumine. *Radiopaedia*. https://radiopaedia.org/articles/gadoterate-meglumine?lang=us (accessed 2022-08-28).
- (35) Gadobutrol. *Radiopaedia*. https://radiopaedia.org/articles/gadobutrol?lang=us (accessed 2022-08-28).
- (36) Gadofosveset trisodium. Radiopaedia. https://radiopaedia.org/articles/gadofosveset-trisodium-1?lang=us (accessed 2022-08-28).
- (37) Gadoxetate disodium. Radiopaedia. https://radiopaedia.org/articles/gadoxetate-disodium?lang=us (accessed 2022-08-28).
- (38) Gadoversetamide. *Radiopaedia*. https://radiopaedia.org/articles/gadoversetamide?lang=us (accessed 2022-08-28).
- (39) Gadopentetate dimeglumine. *Radiopaedia*. https://radiopaedia.org/articles/gadopentetate-dimeglumine?lang=us (accessed 2022-08-28).
- (40) Gadodiamide. *Radiopaedia*. https://radiopaedia.org/articles/gadodiamide?lang=us (accessed 2022-08-28).
- (41) Gadoteridol. *Radiopaedia*. https://radiopaedia.org/articles/gadoteridol?lang=us (accessed 2022-08-28).
- (42) FDA Drug Safety Communication: New warnings for using gadolinium-based contrast agents in patients with kidney dysfunction. FDA. https://www.fda.gov/drugs/drug-safety-and-availability/fda-drug-safety-communication-new-warnings-using-gadolinium-based-contrast-agents-patients-kidney (accessed 2022-11-04).
- (43) Collidge, T. A.; Thomson, P. C.; Mark, P. B.; Traynor, J. P.; Jardine, A. G.; Morris, S. T. W.; Simpson, K.; Roditi, G. H. Gadolinium-Enhanced MR Imaging and Nephrogenic Systemic Fibrosis: Retrospective Study of a Renal Replacement Therapy Cohort. *Radiology* **2007**, 245 (1), 168–175.
- (44) Shamam, Y. M.; De, O. Nephrogenic Systemic Fibrosis Continuing Education Activity. https://www.ncbi.nlm.nih.gov/books/NBK567754/?report=printable.
- (45) FDA Drug Safety Communication: FDA warns that gadolinium-based contrast agents (GBCAs) are retained in the body; requires new class warnings. FDA. https://www.fda.gov/drugs/drug-safety-and-availability/fda-drug-safety-communication-fda-warns-gadolinium-based-contrast-agents-gbcas-are-retained-body (accessed 2022-08-27).
- (46) Guo, B. J.; Yang, Z. L.; Zhang, L. J. Gadolinium Deposition in Brain: Current Scientific Evidence and Future Perspectives. *Frontiers in Molecular Neuroscience* **2018**, DOI: 10.3389/fnmol.2018.00335.

- (47) Soares, S.; Sousa, J.; Pais, A.; Vitorino, C. Nanomedicine: Principles, Properties, and Regulatory Issues. *Frontiers in Chemistry* **2018**, DOI: 10.3389/fchem.2018.00360.
- (48) Patil, R.; Galstyan, A.; Grodzinski, Z. B.; Shatalova, E. S.; Wagner, S.; Israel, L. L.; Ding, H.; Black, K. L.; Ljubimova, J. Y.; Holler, E. Single-and Multi-Arm Gadolinium Mri Contrast Agents for Targeted Imaging of Glioblastoma. *Int. J. Nanomedicine* **2020**, *15*, 3057–3070.
- (49) De, R.; Mahata, M. K.; Kim, K. T. Structure-Based Varieties of Polymeric Nanocarriers and Influences of Their Physicochemical Properties on Drug Delivery Profiles. *Advanced Science* **2022**, 9 (10), 2105373.
- (50) Saraiva, C.; Praça, C.; Ferreira, R.; Santos, T.; Ferreira, L.; Bernardino, L. Nanoparticle-Mediated Brain Drug Delivery: Overcoming Blood-Brain Barrier to Treat Neurodegenerative Diseases. *J. Controlled Release* **2016**, 235, 34–47.
- (51) Prabhu, R. H.; Patravale, V. B.; Joshi, M. D. Polymeric Nanoparticles for Targeted Treatment in Oncology: Current Insights. *International Journal of Nanomedicine* **2015**, 1001–1018.
- (52) Li, Z.; Tan, S.; Li, S.; Shen, Q.; Wang, K. Cancer Drug Delivery in the Nano Era: An Overview and Perspectives (Review). *Oncol. Rep.* **2017**, 611–624.
- (53) Jerbić, I. Š. Biodegradable Synthetic Polymers and Their Application in Advanced Drug Delivery Systems (DDS). *Nanotechnology & Applications* **2018**, *1* (1), 1–9.
- (54) Ulbrich, K.; Holá, K.; Šubr, V.; Bakandritsos, A.; Tuček, J.; Zbořil, R. Targeted Drug Delivery with Polymers and Magnetic Nanoparticles: Covalent and Noncovalent Approaches, Release Control, and Clinical Studies. *Chemical Reviews* **2016**, 5338–5431.
- (55) Liechty, W. B.; Kryscio, D. R.; Slaughter, B. v.; Peppas, N. A. Polymers for Drug Delivery Systems. *Annu. Rev. Chem. Biomol Eng.* **2010**, *1*, 149–173.
- (56) Sung, Y. K.; Kim, S. W. Recent Advances in Polymeric Drug Delivery Systems. *Biomaterials Research* **2020**, DOI: 10.1186/s40824-020-00190-7.
- (57) Jurak, M.; Wiącek, A. E.; Ładniak, A.; Przykaza, K.; Szafran, K. What Affects the Biocompatibility of Polymers? *Adv. Colloid Interface Sci.* **2021**, DOI: 10.1016/j.cis.2021.102451.
- (58) Ribovski, L.; Hamelmann, N. M.; Paulusse, J. M. J. Polymeric Nanoparticles Properties and Brain Delivery. *Pharmaceutics* **2021**, DOI: 10.3390/pharmaceutics13122045.
- (59) Annu; Sartaj, A.; Qamar, Z.; Md, S.; Alhakamy, N. A.; Baboota, S.; Ali, J. An Insight to Brain Targeting Utilizing Polymeric Nanoparticles: Effective Treatment Modalities for Neurological Disorders and Brain Tumor. *Frontiers in Bioengineering and Biotechnology* **2022**, DOI: 10.3389/fbioe.2022.788128.
- (60) Carroll, M. R. J.; Huffstetler, P. P.; Miles, W. C.; Goff, J. D.; Davis, R. M.; Riffle, J. S.; House, M. J.; Woodward, R. C.; St Pierre, T. G. The Effect of Polymer Coatings on Proton Transverse Relaxivities of Aqueous Suspensions of magnetic Nanoparticles. *Nanotechnology* **2011**, 22 (32), 325702.
- (61) Fu, C.; Duan, X.; Cao, M.; Jiang, S.; Ban, X.; Guo, N.; Zhang, F.; Mao, J.; Huyan, T.; Shen, J.; Zhang, L. M. Targeted Magnetic Resonance Imaging and Modulation of Hypoxia with Multifunctional Hyaluronic Acid-MnO2 Nanoparticles in Glioma. *Adv. Healthc Mater.* **2019**, *8* (10), 1900047.
- (62) Jang, Y. J.; Liu, S.; Yue, H.; Park, J. A.; Cha, H.; Ho, S. L.; Marasini, S.; Ghazanfari, A.; Ahmad, M. Y.; Miao, X.; Tegafaw, T.; Chae, K. S.; Chang, Y.; Lee, G. H. Hydrophilic Biocompatible Poly(Acrylic Acid-Co-Maleic Acid) Polymer as a Surface-Coating Ligand of Ultrasmall Gd2O3 Nanoparticles to Obtain a High R1 Value and T1Mr Images. *Diagnostics* **2021**, *11* (1), 2.
- (63) Ponsiglione, A. M.; Russo, M.; Netti, P. A.; Torino, E. Impact of Biopolymer Matrices on Relaxometric Properties of Contrast Agents. *Interface Focus* **2016**, *6* (6), 20160061.
- (64) Rowe, M. D.; Chang, C. C.; Thamm, D. H.; Kraft, S. L.; Harmon, J. F., Jr.; Vogt, A. P.; Sumerlin, B. S.; Boyes, S. G. Tuning the Magnetic Resonance Imaging Properties of Positive Contrast Agent Nanoparticles by Surface Modification with RAFT Polymers. *Langmuir* **2009**, 25 (16), 9487–9499.

- (65) Karfeld-Sulzer, L. S.; Waters, E. A.; Davis, N. E.; Meade, T. J.; Barron, A. E. Multivalent Protein Polymer Mri Contrast Agents: Controlling Relaxivity via Modulation of Amino Acid Sequence. *Biomacromolecules* **2010**, *11* (6), 1429–1436.
- (66) Osorno, L. L.; Brandley, A. N.; Maldonado, D. E.; Yiantsos, A.; Mosley, R. J.; Byrne, M. E. Review of Contemporary Self-Assembled Systems for the Controlled Delivery of Therapeutics in Medicine. *Nanomaterials* **2021**, 1–28.
- (67) Jaruszewski, K. M.; Curran, G. L.; Swaminathan, S. K.; Rosenberg, J. T.; Grant, S. C.; Ramakrishnan, S.; Lowe, V. J.; Poduslo, J. F.; Kandimalla, K. K. Multimodal Nanoprobes to Target Cerebrovascular Amyloid in Alzheimer's Disease Brain. *Biomaterials* **2014**, 35 (6), 1967–1976.
- (68) Li, J.; Huang, S.; Shao, K.; Liu, Y.; An, S.; Kuang, Y.; Guo, Y.; Ma, H.; Wang, X.; Jiang, C. A Choline Derivate-Modified Nanoprobe for Glioma Diagnosis Using MRI. *Sci. Rep* **2013**, DOI: 10.1038/srep01623.
- (69) Geng, K.; Yang, Z. X.; Huang, D.; Yi, M.; Jia, Y.; Yan, G.; Cheng, X.; Wu, R. Tracking of Mesenchymal Stem Cells Labeled with Gadolinium Diethylenetriamine Pentaacetic Acid by 7T Magnetic Resonance Imaging in a Model of Cerebral Ischemia. *Mol. Med. Rep* 2015, 11 (2), 954–960.
- (70) Wang, Z.; Zhou, X.; Xu, Y.; Fan, S.; Tian, N.; Zhang, W.; Sheng, F.; Lin, J.; Zhong, W. Development of a Novel Dual-Order Protein-Based Nanodelivery Carrier That Rapidly Targets Low-Grade Gliomas with Microscopic Metastasis in Vivo. ACS Omega 2020, 5 (32), 20653—20663
- (71) Du, Y.; Qian, M.; Li, C.; Jiang, H.; Yang, Y.; Huang, R. Facile Marriage of Gd3+ to Polymer-Coated Carbon Nanodots with Enhanced Biocompatibility for Targeted MR/Fluorescence Imaging of Glioma. *Int. J. Pharm.* **2018**, 552 (1–2), 84–90.
- (72) Cahalane, C.; Bonezzi, J.; Shelestak, J.; Clements, R.; Boika, A.; Yun, Y. H.; Shriver, L. P. Targeted Delivery of Anti-Inflammatory and Imaging Agents to Microglial Cells with Polymeric Nanoparticles. *Mol. Pharmaceutics* **2020**, *17* (6), 1816–1826.
- (73) Verry, C.; Dufort, S.; Lemasson, B.; Grand, S.; Pietras, J.; Troprès, I.; Crémillieux, Y.; Lux, F.; Mériaux, S.; Larrat, B.; Balosso, J.; le Duc, G.; Barbier, E. L.; Tillement, O. Targeting Brain Metastases with Ultrasmall Theranostic Nanoparticles, a First-in-Human Trial from an MRI Perspective. *Sci. Adv.* **2020**, *6* (29), eaay5279.
- (74) Radiotherapy of Multiple Brain Metastases Using AGuIX. *ClinicalTrials.gov*. https://clinicaltrials.gov/ct2/show/NCT03818386 (accessed 2022-08-28).
- (75) Shen, Z.; Liu, T.; Yang, Z.; Zhou, Z.; Tang, W.; Fan, W.; Liu, Y.; Mu, J.; Li, L.; Bregadze, V. I.; Mandal, S. K.; Druzina, A. A.; Wei, Z.; Qiu, X.; Wu, A.; Chen, X. Small-Sized Gadolinium Oxide Based Nanoparticles for High-Efficiency Theranostics of Orthotopic Glioblastoma. *Biomaterials* **2020**, 235, 119783.
- (76) Du, Y.; Qian, M.; Li, C.; Jiang, H.; Yang, Y.; Huang, R. Facile Marriage of Gd3+ to Polymer-Coated Carbon Nanodots with Enhanced Biocompatibility for Targeted MR/Fluorescence Imaging of Glioma. *Int. J. Pharm.* **2018**, *552* (1–2), 84–90.
- (77) Jeon, M.; Halbert, M. v.; Stephen, Z. R.; Zhang, M. Iron Oxide Nanoparticles as T1 Contrast Agents for Magnetic Resonance Imaging: Fundamentals, Challenges, Applications, and Prospectives. *Adv. Mater.* **2021**, DOI: 10.1002/adma.201906539.
- (78) Costagliola di Polidoro, A.; Zambito, G.; Haeck, J.; Mezzanotte, L.; Lamfers, M.; Netti, P. A.; Torino, E. Theranostic Design of Angiopep-2 Conjugated Hyaluronic Acid Nanoparticles (Thera-angchanps) for Dual Targeting and Boosted Imaging of Glioma Cells. *Cancers (Basel)* **2021**, *13* (3), 503.
- (79) Jin, Y.; Li, Y.; Yang, X.; Tian, J. Neuroblastoma-Targeting Triangular Gadolinium Oxide Nanoplates for Precise Excision of Cancer. *Acta Biomater* **2019**, *87*, 223–234.
- (80) Luo, Y.; Kim, E. H.; Flask, C. A.; Clark, H. A. Nanosensors for the Chemical Imaging of Acetylcholine Using Magnetic Resonance Imaging. *ACS Nano* **2018**, *12* (6), 5761–5773.
- (81) Tedla, G.; Plotkin, J.; Dellinger, A.; Kepley, C. Design and Testing of Dual-Targeted Gd3N@C80-Containing Glioblastoma Theranostics. *J. Nanomater* **2019**.

- (82) Feng, G.; Li, J. L. Y.; Claser, C.; Balachander, A.; Tan, Y.; Goh, C. C.; Kwok, I. W. H.; Rénia, L.; Tang, B. Z.; Ng, L. G.; Liu, B. Dual Modal Ultra-Bright Nanodots with Aggregation-Induced Emission and Gadolinium-Chelation for Vascular Integrity and Leakage Detection. *Biomaterials* **2018**, *152*, 77–85.
- (83) Dong, X.; Ding, Y.; Wu, P.; Wang, C.; Schäfer, C. G. Preparation of MRI-Visible Gadolinium Methacrylate Nanoparticles with Low Cytotoxicity and High Magnetic Relaxivity. *J. Mater. Sci.* **2017**, *52* (13), 7625–7636.
- (84) Chen, D.; Zhou, Y.; Yang, D.; Guan, M.; Zhen, M.; Lu, W.; van Dort, M. E.; Ross, B. D.; Wang, C.; Shu, C.; Hong, H. Positron Emission Tomography/Magnetic Resonance Imaging of Glioblastoma Using a Functionalized Gadofullerene Nanoparticle. *ACS Appl. Mater. Interfaces* **2019**, *11* (24), 21343–21352.
- (85) Hashempour Alamdari, N.; Alaei-Beirami, M.; Sadat Shandiz, S. A.; Hejazinia, H.; Rasouli, R.; Saffari, M.; Sadat Ebrahimi, S. E.; Assadi, A.; Shafiee Ardestani, M. Gd3+-Asparagine-Anionic Linear Globular Dendrimer Second-Generation G2 Complexes: Novel Nanobiohybrid Theranostics. *Contrast Media Mol. Imaging* **2017**, 3625729.
- (86) Samanta, S.; le Joncour, V.; Wegrzyniak, O.; Rangasami, V. K.; Ali-Löytty, H.; Hong, T.; Selvaraju, R. K.; Aberg, O.; Hilborn, J.; Laakkonen, P.; Varghese, O. P.; Eriksson, O.; Cabral, H.; Oommen, O. P. Heparin-Derived Theranostic Nanoprobes Overcome the Blood–Brain Barrier and Target Glioma in Murine Model. *Adv. Ther (Weinh)* **2022**, *5* (6), 2200001.
- (87) Dufort, S.; Appelboom, G.; Verry, C.; Barbier, E. L.; Lux, F.; Bräuer-Krisch, E.; Sancey, L.; Chang, S. D.; Zhang, M.; Roux, S.; Tillement, O.; le Duc, G. Ultrasmall Theranostic Gadolinium-Based Nanoparticles Improve High-Grade Rat Glioma Survival. *Journal of Clinical Neuroscience* **2019**, *67*, 215–219.
- (88) Wang, X.; Liu, G.; Chen, N.; Wu, J.; Zhang, J.; Qian, Y.; Zhang, L.; Zhou, D.; Yu, Y. Angiopep2-Conjugated Star-Shaped Polyprodrug Amphiphiles for Simultaneous Glioma-Targeting Therapy and MR Imaging. ACS Appl. Mater. Interfaces 2020, 12 (10), 12143–12154.
- (89) Xu, D.; Baidya, A.; Deng, K.; Li, Y. S.; Wu, B.; Xu, H. B. Multifunctional Nanoparticle PEG-Ce6-Gd for MRI-Guided Photodynamic Therapy. *Oncol. Rep.* **2020**, 45 (2), 547–556.
- (90) Zhang, L.; Chen, D.; Zhang, J.; Cai, R.; Xu, L.; Yu, N.; Zhang, S.; Yan, H.; Jiang, J.; Du, F.; Gong, A. A Novel Cholchicine/Gadolinium-Loading Tubulin Self-Assembly Nanocarrier for MR Imaging and Chemotherapy of Glioma. *Nanotechnology* **2020**, *31* (25), 255601.
- (91) Zhao, Z.; Xu, K.; Fu, C.; Liu, H.; Lei, M.; Bao, J.; Fu, A.; Yu, Y.; Zhang, W. Interfacial Engineered Gadolinium Oxide Nanoparticles for Magnetic Resonance Imaging Guided Microenvironment-Mediated Synergetic Chemodynamic/Photothermal Therapy. *Biomaterials* **2019**, 219, 119379.
- (92) Gries, M.; Thomas, N.; Daouk, J.; Rocchi, P.; Choulier, L.; Jubréaux, J.; Pierson, J.; Reinhard, A.; Jouan-Hureaux, V.; Chateau, A.; Acherar, S.; Frochot, C.; Lux, F.; Tillement, O.; Barberi-Heyob, M. Multiscale Selectivity and in Vivo Biodistribution of Nrp-1-Targeted Theranostic Aguix Nanoparticles for Pdt of Glioblastoma. *Int. J. Nanomedicine* 2020, 15, 8739–8758.
- (93) Bony, B. A.; Miller, H. A.; Tarudji, A. W.; Gee, C. C.; Sarella, A.; Nichols, M. G.; Kievit, F. M. Ultrasmall Mixed Eu-Gd Oxide Nanoparticles for Multimodal Fluorescence and Magnetic Resonance Imaging of Passive Accumulation and Retention in TBI. ACS Omega 2020, 5 (26), 16220–16227.
- (94) Mpambani, F.; Aslund, A. K. O.; Lerouge, F.; Nyström, S.; Reitan, N.; Huuse, E. M.; Widerøe, M.; Chaput, F.; Monnereau, C.; Andraud, C.; Lecouvey, M.; Handrick, S.; Prokop, S.; Heppner, F. L.; Nilsson, P.; Hammarström, P.; Lindgren, M.; Parola, S. Two-Photon Fluorescence and Magnetic Resonance Specific Imaging of $A\beta$ Amyloid Using Hybrid Nano-GdF3 Contrast Media. *ACS Appl. Bio Mater.* **2018**, 1 (2), 462–472.
- (95) Xiao, X.; Cai, H.; Huang, Q.; Wang, B.; Wang, X.; Luo, Q.; Li, Y.; Zhang, H.; Gong, Q.; Ma, X.; Gu, Z.; Luo, K. Polymeric Dual-Modal Imaging Nanoprobe with Two-Photon Aggregation-Induced Emission for Fluorescence Imaging and Gadolinium-Chelation for Magnetic Resonance Imaging. *Bioact Mater.* 2023, 19, 538–549.

- (96) Gholibegloo, E.; Ebrahimpour, A.; Mortezazadeh, T.; Sorouri, F.; Foroumadi, A.; Firoozpour, L.; Shafiee Ardestani, M.; Khoobi, M. PH-Responsive Chitosan-Modified Gadolinium Oxide Nanoparticles Delivering 5-Aminolevulinic Acid: A Dual Cellular and Metabolic T1-T2* Contrast Agent for Glioblastoma Brain Tumors Detection. *J. Mol. Lig.* **2022**, *368*, 120628.
- (97) Ling, D.; Hyeon, T. Chemical Design of Biocompatible Iron Oxide Nanoparticles for Medical Applications. *Small* **2013**, *9*, 1450–1466.
- (98) Lee, N.; Yoo, D.; Ling, D.; Cho, M. H.; Hyeon, T.; Cheon, J. Iron Oxide Based Nanoparticles for Multimodal Imaging and Magnetoresponsive Therapy. *Chemical Reviews* **2015**, 10637–10689, DOI: 10.1021/acs.chemrev.5b00112.
- (99) Stroh, A.; Zimmer, C.; Gutzeit, C.; Jakstadt, M.; Marschinke, F.; Jung, T.; Pilgrimm, H.; Grune, T. Iron Oxide Particles for Molecular Magnetic Resonance Imaging Cause Transient Oxidative Stress in Rat Macrophages. *Free Radic Biol. Med.* **2004**, *36* (8), 976–984.
- (100) Blasiak, B.; van Veggel, F. C. J. M.; Tomanek, B. Applications of Nanoparticles for MRI Cancer Diagnosis and Therapy. *J. Nanomater.* **2013**, 2013, 1.
- (101) Shen, Z.; Wu, A.; Chen, X. Iron Oxide Nanoparticle Based Contrast Agents for Magnetic Resonance Imaging. *Molecular Pharmaceutics* **2017**, 1352–1364, DOI: 10.1021/acs.molpharmaceut.6b00839.
- (102) Avasthi, A.; Caro, C.; Pozo-Torres, E.; Leal, M. P.; García-Martín, M. L. Magnetic Nanoparticles as MRI Contrast Agents. *Topics in Current Chemistry*; Springer Science and Business Media Deutschland GmbH, June 1, 2020. DOI: 10.1007/s41061-020-00302-w.
- (103) Jun, Y. W.; Seo, J. W.; Cheon, J. Nanoscaling Laws of Magnetic Nanoparticles and Their Applicabilities in Biomedical Sciences. *Acc. Chem. Res.* **2008**, *41* (2), 179–189.
- (104) Li, D.; Shen, M.; Xia, J.; Shi, X. Recent Developments of Cancer Nanomedicines Based on Ultrasmall Iron Oxide Nanoparticles and Nanoclusters. *Nanomedicine* **2021**, 609–612.
- (105) Wu, L.; Wen, W.; Wang, X.; Huang, D.; Cao, J.; Qi, X.; Shen, S. Ultrasmall Iron Oxide Nanoparticles Cause Significant Toxicity by Specifically Inducing Acute Oxidative Stress to Multiple Organs. *Part Fibre Toxicol* **2022**, DOI: 10.1186/s12989-022-00465-y.
- (106) Chee, H. L.; Gan, C. R. R.; Ng, M.; Low, L.; Fernig, D. G.; Bhakoo, K. K.; Paramelle, D. Biocompatible Peptide-Coated Ultrasmall Superparamagnetic Iron Oxide Nanoparticles for in Vivo Contrast-Enhanced Magnetic Resonance Imaging. *ACS Nano* **2018**, *12* (7), 6480–6491.
- (107) Roca, A. G.; Gutiérrez, L.; Gavilán, H.; Fortes Brollo, M. E.; Veintemillas-Verdaguer, S.; Morales, M. del P. Design Strategies for Shape-Controlled Magnetic Iron Oxide Nanoparticles. *Adv. Drug Delivery Rev.* **2019**, 68–104.
- (108) Geppert, M.; Himly, M. Iron Oxide Nanoparticles in Bioimaging An Immune Perspective. *Frontiers in Immunology* **2021**, DOI: 10.3389/fimmu.2021.688927.
- (109) Wei, H.; Wi Sniowska B, A.; Fan, J.; Harvey, P.; Li, Y.; Wu, V.; Hansen, E. C.; Zhang, J.; Kaul, M. G.; Frey, A. M.; Adam, G.; Frenkel, A. I.; Bawendi, M. G.; Jasanoff, A. Single-Nanometer Iron Oxide Nanoparticles as Tissue-Permeable MRI Contrast Agents. *PNAS* **2021**, *118* (42), e2102340118.
- (110) Du, C.; Wang, J.; Liu, X.; Li, H.; Geng, D.; Yu, L.; Chen, Y.; Zhang, J. Construction of Pepstatin A-Conjugated Ultrasmall SPIONs for Targeted Positive MR Imaging of Epilepsy-Overexpressed P-Glycoprotein. *Biomaterials* **2020**, 230, 119581.
- (111) Sukumar, U. K.; Bose, R. J. C.; Malhotra, M.; Babikir, H. A.; Afjei, R.; Robinson, E.; Zeng, Y.; Chang, E.; Habte, F.; Sinclair, R.; Gambhir, S. S.; Massoud, T. F.; Paulmurugan, R. Intranasal Delivery of Targeted Polyfunctional Gold—Iron Oxide Nanoparticles Loaded with Therapeutic MicroRNAs for Combined Theranostic Multimodality Imaging and Presensitization of Glioblastoma to Temozolomide. *Biomaterials* **2019**, *218*, 119342.
- (112) Suárez-García, S.; Arias-Ramos, N.; Frias, C.; Candiota, A. P.; Arús, C.; Lorenzo, J.; Ruiz-Molina, D.; Novio, F. Dual T1/ T2 Nanoscale Coordination Polymers as Novel Contrast Agents for MRI:

- A Preclinical Study for Brain Tumor. ACS Appl. Mater. Interfaces 2018, 10 (45), 38819–38832.
- (113) Amendola, V.; Guadagnini, A.; Agnoli, S.; Badocco, D.; Pastore, P.; Fracasso, G.; Gerosa, M.; Vurro, F.; Busato, A.; Marzola, P. Polymer-Coated Silver-Iron Nanoparticles as Efficient and Biodegradable MRI Contrast Agents. *J. Colloid Interface Sci.* 2021, 596, 332–341.
- (114) Das, P.; Salvioni, L.; Malatesta, M.; Vurro, F.; Mannucci, S.; Gerosa, M.; Antonietta Rizzuto, M.; Tullio, C.; Degrassi, A.; Colombo, M.; Ferretti, A. M.; Ponti, A.; Calderan, L.; Prosperi, D. Colloidal Polymer-Coated Zn-Doped Iron Oxide Nanoparticles with High Relaxivity and Specific Absorption Rate for Efficient Magnetic Resonance Imaging and Magnetic Hyperthermia. *J. Colloid Interface Sci.* 2020, 579, 186–194.
- (115) Fernández-Barahona, I.; Gutiérrez, L.; Veintemillas-Verdaguer, S.; Pellico, J.; Morales, M. D. P.; Catala, M.; del Pozo, M. A.; Ruiz-Cabello, J.; Herranz, F. Cu-Doped Extremely Small Iron Oxide Nanoparticles with Large Longitudinal Relaxivity: One-Pot Synthesis and in Vivo Targeted Molecular Imaging. ACS Omega 2019, 4 (2), 2719–2727.
- (116) Yang, L.; Fu, S.; Cai, Z.; Liu, L.; Xia, C.; Gong, Q.; Song, B.; Ai, H. Integration of PEG-Conjugated Gadolinium Complex and Superparamagnetic Iron Oxide Nanoparticles as T 1— T 2 Dual-Mode Magnetic Resonance Imaging Probes. Regen Biomater 2021, DOI: 10.1093/rb/rbab064.
- (117) Barajas, R. F.; Hamilton, B. E.; Schwartz, D.; Mcconnell, H. L.; Pettersson, D. R.; Horvath, A.; Szidonya, L.; Varallyay, C. G.; Firkins, J.; Jaboin, J. J.; Kubicky, C. D.; Raslan, A. M.; Dogan, A.; Cetas, J. S.; Ciporen, J.; Han, S. J.; Ambady, P.; Muldoon, L. L.; Woltjer, R.; Rooney, W. D.; Neuwelt, E. A. Combined Iron Oxide Nanoparticle Ferumoxytol and Gadolinium Contrast Enhanced MRI Define Glioblastoma Pseudoprogression. *Neuro Oncol* 2019, 21 (4), 517–526. (118) Xiao, S.; Yu, X.; Zhang, L.; Zhang, Y.; Fan, W.; Sun, T.; Zhou, C.; Liu, Y.; Liu, Y.; Gong, M.; Zhang, D. Synthesis of Peg-Coated, Ultrasmall, Manganese-Doped Iron Oxide Nanoparticles with High Relaxivity for T1 /T2 Dual-Contrast Magnetic Resonance Imaging. *Int. J. Nanomedicine* 2019, 14, 8499–8507.
- (119) Chouhan, R. S.; Horvat, M.; Ahmed, J.; Alhokbany, N.; Alshehri, S. M.; Gandhi, S. Magnetic Nanoparticles—A Multifunctional Potential Agent for Diagnosis and Therapy. *Cancers* **2021**, DOI: 10.3390/cancers13092213.
- (120) Chen, W.; Xu, Y.; Yang, D.; Wang, P.; Xu, Y.; Zhu, J.; Cui, D. Preparation of Liposomes Coated Superparamagnetic Iron Oxide Nanoparticles for Targeting and Imaging Brain Glioma. *Nano Biomed Eng.* **2022**, *14* (1), 71–80.
- (121) Zhang, X.; Zhou, J.; Gu, Z.; Zhang, H.; Gong, Q.; Luo, K. Advances in Nanomedicines for Diagnosis of Central Nervous System Disorders. *Biomaterials* **2021**, DOI: 10.1016/j.biomaterials.2020.120492.
- (122) Chen, B.; Guo, Z.; Guo, C.; Mao, Y.; Qin, Z.; Ye, D.; Zang, F.; Lou, Z.; Zhang, Z.; Li, M.; Liu, Y.; Ji, M.; Sun, J.; Gu, N. Moderate Cooling Coprecipitation for Extremely Small Iron Oxide as a PH Dependent: T 1-MRI Contrast Agent. *Nanoscale* **2020**, *12* (9), 5521–5532
- (123) Xie, M.; Li, Y.; Xu, Y.; Zhang, Z.; Ji, B.; Jones, J. B.; Wang, Z.; Mao, H. Brain Tumor Imaging and Delivery of Sub-5 Nm Magnetic Iron Oxide Nanoparticles in an Orthotopic Murine Model of Glioblastoma. ACS Appl. Nano Mater. 2022, 5, 9706.
- (124) Shen, C.; Wang, X.; Zheng, Z.; Gao, C.; Chen, X.; Zhao, S.; Dai, Z. Doxorubicin and Indocyanine Green Loaded Superparamagnetic Iron Oxide Nanoparticles with PEGylated Phospholipid Coating for Magnetic Resonance with Fluorescence Imaging and Chemotherapy of Glioma. *Int. J. Nanomedicine* **2019**, *14*, 101–117.
- (125) Li, Y.; Xie, M.; Jones, J. B.; Zhang, Z.; Wang, Z.; Dang, T.; Wang, X.; Lipowska, M.; Mao, H. Targeted Delivery of DNA Topoisomerase Inhibitor SN38 to Intracranial Tumors of Glioblastoma Using Sub-5 Ultrafine Iron Oxide Nanoparticles. *Adv. Healthc Mater.* 2022, 11 (14), 2102816.
- (126) Wei, R.; Liu, Y.; Gao, J.; Yong, V. W.; Xue, M. Small Functionalized Iron Oxide Nanoparticles for Dual Brain Magnetic

- Resonance Imaging and Fluorescence Imaging. RSC Adv. 2021, 11 (21), 12867–12875.
- (127) Waddington, D. E. J.; Boele, T.; Maschmeyer, R.; Kuncic, Z.; Rosen, M. S. High-Sensitivity in Vivo Contrast for Ultra-Low Field Magnetic Resonance Imaging Using Superparamagnetic Iron Oxide Nanoparticles. *Sci. Adv.* **2020**, *6* (29), eabb0998.
- (128) Wang, X.; Chen, L.; Ge, J.; Afshari, M. J.; Yang, L.; Miao, Q.; Duan, R.; Cui, J.; Liu, C.; Zeng, J.; Zhong, J.; Gao, M. Rational Constructed Ultra-Small Iron Oxide Nanoprobes Manifesting High Performance for T 1-Weighted Magnetic Resonance Imaging of Glioblastoma. *Nanomaterials* **2021**, *11*, 2601.
- (129) Torkashvand, N.; Sarlak, N. Fabrication of a Dual T1 and T2 Contrast Agent for Magnetic Resonance Imaging Using Cellulose Nanocrystals/Fe3O4 Nanocomposite. *Eur. Polym. J.* **2019**, *118*, 128–136.
- (130) Xue, X.; Bo, R.; Qu, H.; Jia, B.; Xiao, W.; Yuan, Y.; Vapniarsky, N.; Lindstrom, A.; Wu, H.; Zhang, D.; Li, L.; Ricci, M.; Ma, Z.; Zhu, Z.; Lin, T.-y.; Louie, A. Y.; Li, Y. A Nephrotoxicity-Free, Iron-Based Contrast Agent for Magnetic Resonance Imaging of Tumors. *Biomaterials* **2020**, 257, 120234.
- (131) Wang, C.; Sun, W.; Zhang, J.; Zhang, J.; Guo, Q.; Zhou, X.; Fan, D.; Liu, H.; Qi, M.; Gao, X.; Xu, H.; Gao, Z.; Tian, M.; Zhang, H.; Wang, J.; Wei, Z.; Long, N. J.; Mao, Y.; Li, C. An Electric-Field-Responsive Paramagnetic Contrast Agent Enhances the Visualization of Epileptic Foci in Mouse Models of Drug-Resistant Epilepsy. *Nat. Biomed Eng.* **2021**, 5 (3), 278–289.
- (132) Sherwood, J.; Rich, M.; Lovas, K.; Warram, J.; Bolding, M. S.; Bao, Y. T 1-Enhanced MRI-Visible Nanoclusters for Imaging-Guided Drug Delivery. *Nanoscale* **2017**, *9* (32), 11785–11792.
- (133) Shin, T. H.; Kim, P. K.; Kang, S.; Cheong, J.; Kim, S.; Lim, Y.; Shin, W.; Jung, J. Y.; Lah, J. D.; Choi, B. W.; Cheon, J. High-Resolution T 1 MRI via Renally Clearable Dextran Nanoparticles with an Iron Oxide Shell. *Nat. Biomed Eng.* **2021**, *5* (3), 252–263.
- (134) Horning, K. J.; Caito, S. W.; Tipps, K. G.; Bowman, A. B.; Aschner, M. Manganese Is Essential for Neuronal Health. *Annual Review of Nutrition* **2015**, 71–108, DOI: 10.1146/annurev-nutr-071714-034419.
- (135) Jiang, S.; Li, X.; Zhang, F.; Mao, J.; Cao, M.; Zhang, X.; Huang, S.; Duan, X.; Shen, J. Manganese Dioxide-Based Nanocarrier Delivers Paclitaxel to Enhance Chemotherapy against Orthotopic Glioma through Hypoxia Relief. *Small Methods* **2022**, *6*, 2101531.
- (136) Daksh, S.; Kaul, A.; Deep, S.; Datta, A. Current Advancement in the Development of Manganese Complexes as Magnetic Resonance Imaging Probes. *Journal of Inorganic Biochemistry* **2022**, 112018.
- (137) Harischandra, D. S.; Ghaisas, S.; Zenitsky, G.; Jin, H.; Kanthasamy, A.; Anantharam, V.; Kanthasamy, A. G. Manganese-Induced Neurotoxicity: New Insights into the Triad of Protein Misfolding, Mitochondrial Impairment, and Neuroinflammation. *Frontiers in Neuroscience* **2019**, DOI: 10.3389/fnins.2019.00654.
- (138) Manganese chloride tetrahydrate | $\text{Cl}_2\text{H}_8\text{MnO}_4$. PubChem. https://pubchem.ncbi.nlm.nih.gov/compound/Manganese-chloridetetrahydrate (accessed 2022-08-28).
- (139) Teslascan (Mangafodipir): Uses, Dosage, Side Effects, Interactions, Warning. RxList. https://www.rxlist.com/teslascan-drug.htm (accessed 2022-08-28).
- (140) Sobańska, Z.; Roszak, J.; Kowalczyk, K.; Stępnik, M. Applications and Biological Activity of Nanoparticles of Manganese and Manganese Oxides in in Vitro and in Vivo Models. *Nanomaterials* **2021**, DOI: 10.3390/nano11051084.
- (141) García-Hevia, L.; Bañobre-López, M.; Gallo, J. Recent Progress on Manganese-Based Nanostructures as Responsive MRI Contrast Agents. *Chem.-Eur. J.* **2019**, 431–441.
- (142) Zhen, Z.; Xie, J. Development of Manganese-Based Nanoparticles as Contrast Probes for Magnetic Resonance Imaging. *Theranostics* **2012**, *2*, 45–54.
- (143) Shin, J.; Anisur, R. M.; Ko, M. K.; Im, G. H.; Lee, J. H.; Lee, I. S. Hollow Manganese Oxide Nanoparticles as Multifunctional Agents for Magnetic Resonance Imaging and Drug Delivery. *Angewandte Chemie International Edition* **2009**, 48 (2), 321–324.

- (144) Jun, Y. W.; Huh, Y. M.; Choi, J. S.; Lee, J. H.; Song, H. T.; Kim, S.; Yoon, S.; Kim, K. S.; Shin, J. S.; Suh, J. S.; Cheon, J. Nanoscale Size Effect of Magnetic Nanocrystals and Their Utilization for Cancer Diagnosis via Magnetic Resonance Imaging. *J. Am. Chem. Soc.* **2005**, 127 (16), 5732–5733.
- (145) Hsu, B. Y. W.; Kirby, G.; Tan, A.; Seifalian, A. M.; Li, X.; Wang, J. Relaxivity and Toxicological Properties of Manganese Oxide Nanoparticles for MRI Applications. *RSC Advances* **2016**, 45462–45474.
- (146) Martinez de la Torre, C.; Grossman, J. H.; Bobko, A. A.; Bennewitz, M. F. Tuning the Size and Composition of Manganese Oxide Nanoparticles through Varying Temperature Ramp and Aging Time. *PLoS One* **2020**, *15*, e0239034.
- (147) An, K.; Park, M.; Yu, J. H.; Na, H. B.; Lee, N.; Park, J.; Choi, S. H.; Song, I. C.; Moon, W. K.; Hyeon, T. Synthesis of Uniformly Sized Manganese Oxide Nanocrystals with Various Sizes and Shapes and Characterization of Their T 1 Magnetic Resonance Relaxivity. *Eur. J. Inorg. Chem.* **2012**, 2012 (12), 2148–2155.
- (148) García-Hevia, L.; Bañobre-López, M.; Gallo, J. Recent Progress on Manganese-Based Nanostructures as Responsive MRI Contrast Agents. *Chem.-Eur. J.* **2019**, 431–441.
- (149) Jiang, X.; Gray, P.; Patel, M.; Zheng, J.; Yin, J. J. Crossover between Anti- And pro-Oxidant Activities of Different Manganese Oxide Nanoparticles and Their Biological Implications. *J. Mater. Chem. B* **2020**, *8* (6), 1191–1201.
- (150) Sun, D.; Liu, K.; Li, Y.; Xie, T.; Zhang, M.; Liu, Y.; Tong, H.; Guo, Y.; Zhang, Q.; Liu, H.; Fang, J.; Chen, X. Intrinsically Bioactive Manganese—Eumelanin Nanocomposites Mediated Antioxidation and Anti-Neuroinflammation for Targeted Theranostics of Traumatic Brain Injury. Adv. Healthc Mater. 2022, 11, 2200517.
- (151) Lee, J.; Kumari, N.; Kim, S. M.; Kim, S.; Jeon, K. W.; Im, G. H.; Jang, M. S.; Lee, W. J.; Lee, J. H.; Lee, I. S. Anchoring Ligand-Effect on Bright Contrast-Enhancing Property of Hollow Mn3O4 Nanoparticle in T1-Weighted Magnetic Resonance Imaging. *Chem. Mater.* **2018**, *30* (12), 4056–4064.
- (152) Tan, J.; Duan, X.; Zhang, F.; Ban, X.; Mao, J.; Cao, M.; Han, S.; Shuai, X.; Shen, J. Theranostic Nanomedicine for Synergistic Chemodynamic Therapy and Chemotherapy of Orthotopic Glioma. *Advanced Science* **2020**, *7* (24), 2003036.
- (153) Marasini, S.; Yue, H.; Ho, S.-L.; Park, J.-A.; Kim, S.; Yang, J.-U.; Cha, H.; Liu, S.; Tegafaw, T.; Ahmad, M. Y.; Saidi, A. K. A. A.; Zhao, D.; Liu, Y.; Chae, K.-S.; Chang, Y.; Lee, G.-H. In Vivo Positive Magnetic Resonance Imaging of Brain Cancer (U87MG) Using Folic Acid-Conjugated Polyacrylic Acid-Coated Ultrasmall Manganese Oxide Nanoparticles. *Applied Sciences (Switzerland)* **2021**, *11* (6), 2596.
- (154) Huang, W. C.; Lo, Y. C.; Chu, C. Y.; Lai, H. Y.; Chen, Y. Y.; Chen, S. Y. Conductive Nanogel-Interfaced Neural Microelectrode Arrays with Electrically Controlled in-Situ Delivery of Manganese Ions Enabling High-Resolution MEMRI for Synchronous Neural Tracing with Deep Brain Stimulation. *Biomaterials* **2017**, *122*, 141–153.
- (155) Mauri, M.; Collico, V.; Morelli, L.; Das, P.; García, I.; Penaranda Avila, J.; Bellini, M.; Rotem, R.; Truffi, M.; Corsi, F.; Simonutti, R.; Liz-Marzán, L. M.; Colombo, M.; Prosperi, D. MnO Nanoparticles Embedded in Functional Polymers as T1 Contrast Agents for Magnetic Resonance Imaging. ACS Appl. Nano Mater. 2020, 3 (4), 3787–3797. (156) Xu, W.; Zhang, J.; Yang, Z.; Zhao, M.; Long, H.; Wu, Q.; Nian, F. Tannin—Mn Coordination Polymer Coated Carbon Quantum Dots Nanocomposite for Fluorescence and Magnetic Resonance Bimodal Imaging. J. Mater. Sci. Mater. Med. 2022, DOI: 10.1007/s10856-021-06629-0.
- (157) He, C.; Ahmed, T.; Abbasi, A. Z.; Li, L. Y.; Foltz, W. D.; Cai, P.; Knock, E.; Fraser, P. E.; Rauth, A. M.; Henderson, J. T.; Wu, X. Y. Multifunctional Bioreactive-Nanoconstructs for Sensitive and Accurate MRI of Cerebrospinal Fluid Pathology and Intervention of Alzheimer's Disease. *Nano Today* **2020**, *35*, 100965.
- (158) Sanchez-Ramos, J.; Song, S.; Kong, X.; Foroutan, P.; Martinez, G.; Dominguez-Viqueria, W.; Mohapatra, S.; Mohapatra, S.; Haraszti, R. A.; Khvorova, A.; Aronin, N.; Sava, V. Chitosan-Mangafodipir

Review

- Nanoparticles Designed for Intranasal Delivery of SiRNA and DNA to Brain. *J. Drug Deliv Sci. Technol.* **2018**, *43*, 453–460.
- (159) Zhang, X.; Zhou, J.; Gu, Z.; Zhang, H.; Gong, Q.; Luo, K. Advances in Nanomedicines for Diagnosis of Central Nervous System Disorders. *Biomaterials* **2021**, DOI: 10.1016/j.biomaterials.2020.120492.
- (160) Soo Choi, H.; Liu, W.; Misra, P.; Tanaka, E.; Zimmer, J. P.; Itty Ipe, B.; Bawendi, M. G.; Frangioni, J. v. Renal Clearance of Quantum Dots. *Nat. Biotechnol.* **2007**, 25 (10), 1165–1170.
- (161) Spencer, B. J.; Verma, I. M. Targeted Delivery of Proteins across the Blood-Brain Barrier. *PNAS* **2007**, *104*, 7594.
- (162) Yamazaki, Y.; Zhao, N.; Caulfield, T. R.; Liu, C. C.; Bu, G. Apolipoprotein E and Alzheimer Disease: Pathobiology and Targeting Strategies. *Nature Reviews Neurology* **2019**, 501–518.
- (163) Neves, A. R.; Queiroz, J. F.; Weksler, B.; Romero, I. A.; Couraud, P. O.; Reis, S. Solid Lipid Nanoparticles as a Vehicle for Brain-Targeted Drug Delivery: Two New Strategies of Functionalization with Apolipoprotein e. *Nanotechnology* **2015**, *26* (49), 495103.
- (164) Kelly, J. M.; Gross, A. L.; Martin, D. R.; Byrne, M. E. Polyethylene Glycol-b-Poly(Lactic Acid) Polymersomes as Vehicles for Enzyme Replacement Therapy. *Nanomedicine* **2017**, *12* (23), 2591–2606
- (165) Zou, Z.; Shao, S.; Zou, R.; Qi, J.; Chen, L.; Zhang, H.; Shen, Q.; Yang, Y.; Ma, L.; Guo, R.; Li, H.; Tian, H.; Li, P.; Yu, M.; Wang, L.; Kong, W.; Li, C.; Yu, Z.; Huang, Y.; Chen, L.; Shao, Q.; Gao, X.; Chen, X.; Zhang, Z.; Yan, J.; Shao, X.; Pan, R.; Xu, L.; Fang, J.; Zhao, L.; Huang, Y.; Li, A.; Zhang, Y.; Huang, W.; Tian, K.; Hu, M.; Xie, L.; Wu, L.; Wu, Y.; Luo, Z.; Xiao, W.; Ma, S.; Wang, J.; Huang, K.; He, S.; Yang, F.; Zhou, S.; Jia, M.; Zhang, H.; Lu, H.; Wang, X.; Tan, J. Linking the Low-Density Lipoprotein Receptor-Binding Segment Enables the Therapeutic S-YHEDA Peptide to Cross the Blood-Brain Barrier and Scavenge Excess Iron and Radicals in the Brain of Senescent Mice. Alzheimer's and Dementia: Translational Research and Clinical Interventions 2019, 5, 717—731.
- (166) Kreuter, J.; Hekmatara, T.; Dreis, S.; Vogel, T.; Gelperina, S.; Langer, K. Covalent Attachment of Apolipoprotein A-I and Apolipoprotein B-100 to Albumin Nanoparticles Enables Drug Transport into the Brain. *J. Controlled Release* **2007**, *118* (1), 54–58.
- (167) Masliah, E.; Spencer, B. Applications of ApoB LDLR-Binding Domain Approach for the Development of CNS-Penetrating Peptides for Alzheimer'Ss Disease. *Methods Mol. Biol.* **2015**, *1324*, 331–337.
- (168) Choudhury, H.; Pandey, M.; Chin, P. X.; Phang, Y. L.; Cheah, J. Y.; Ooi, S. C.; Mak, K. K.; Pichika, M. R.; Kesharwani, P.; Hussain, Z.; Gorain, B. Transferrin Receptors-Targeting Nanocarriers for Efficient Targeted Delivery and Transcytosis of Drugs into the Brain Tumors: A Review of Recent Advancements and Emerging Trends. *Drug Delivery and Translational Research* 2018, 1545–1563.
- (169) Thomsen, M. S.; Johnsen, K. B.; Kucharz, K.; Lauritzen, M.; Moos, T. Blood—Brain Barrier Transport of Transferrin Receptor-Targeted Nanoparticles. *Pharmaceutics* **2022**, DOI: 10.3390/pharmaceutics14102237.
- (170) Zhao, Q.; Du, W.; Zhou, L.; Wu, J.; Zhang, X.; Wei, X.; Wang, S.; Huang, Y.; Li, Y. Transferrin-Enabled Blood—Brain Barrier Crossing Manganese-Based Nanozyme for Rebalancing the Reactive Oxygen Species Level in Ischemic Stroke. *Pharmaceutics* **2022**, *14* (6), 1122.
- (171) Johnsen, K. B.; Burkhart, A.; Thomsen, L. B.; Andresen, T. L.; Moos, T. Targeting the Transferrin Receptor for Brain Drug Delivery. *Progress in Neurobiology* **2019**, DOI: 10.1016/j.pneurobio.2019.101665.
- (172) Ulbrich, K.; Knobloch, T.; Kreuter, J. Targeting the Insulin Receptor: Nanoparticles for Drug Delivery across the Blood-Brain Barrier (BBB). *J. Drug Target* **2011**, *19* (2), 125–132.
- (173) Boado, R. J.; Zhang, Y.; Zhang, Y.; Pardridge, W. M. Humanization of Anti-Human Insulin Receptor Antibody for Drug Targeting across the Human Blood-Brain Barrier. *Biotechnol. Bioeng.* **2007**, *96* (2), 381–391.
- (174) Alata, W.; Yogi, A.; Brunette, E.; Delaney, C. E.; van Faassen, H.; Hussack, G.; Iqbal, U.; Kemmerich, K.; Haqqani, A. S.; Moreno, M. J.; Stanimirovic, D. B. Targeting Insulin-like Growth Factor-1 Receptor

- (IGF1R) for Brain Delivery of Biologics. FASEB J. 2022, 36 (3), e22208.
- (175) Nance, E. A.; Woodworth, G. F.; Sailor, K. A.; Shih, T. Y.; Xu, Q.; Swaminathan, G.; Xiang, D.; Eberhart, C.; Hanes, J. A Dense Poly(Ethylene Glycol) Coating Improves Penetration of Large Polymeric Nanoparticles within Brain Tissue. *Sci. Transl Med.* **2012**, DOI: 10.1126/scitranslmed.3003594.
- (176) Gao, S.; Zhao, L.; Fan, Z.; Kodibagkar, V. D.; Liu, L.; Wang, H.; Xu, H.; Tu, M.; Hu, B.; Cao, C.; Zhang, Z.; Yu, J. X. In Situ Generated Novel 1H MRI Reporter for β -Galactosidase Activity Detection and Visualization in Living Tumor Cells. *Front Chem.* **2021**, DOI: 10.3389/fchem.2021.709581.
- (177) Iqbal, S.; Blenner, M.; Alexander-Bryant, A.; Larsen, J. Polymersomes for Therapeutic Delivery of Protein and Nucleic Acid Macromolecules: From Design to Therapeutic Applications. *Biomacromolecules* **2020**, 1327–1350.
- (178) Discher, D. E.; Ahmed, F. Polymersomes. *Annu. Rev. Biomed Eng.* **2006**, *8* (1), 323–341.